Chapter I
Eigencombining:
A Unified Approach to Antenna Array Signal Processing

Constantin Siriteanu
Seoul National University, Korea

Steven D. Blostein
Queen's University, Canada

ABSTRACT

This chapter unifies the principles and analyses of conventional signal processing algorithms for receive-side smart antennas, and compares their performance and numerical complexity. The chapter starts with a brief look at the traditional single-antenna optimum symbol-detector, continues with analyses of conventional smart antenna algorithms, i.e., statistical beamforming (BF) and maximal-ratio combining (MRC), and culminates with an assessment of their recently-proposed superset known as eigencombining or eigenbeamforming. BF or MRC performance fluctuates with changing propagation conditions, although their numerical complexity remains constant. Maximal-ratio eigencombining (MREC) has been devised to achieve best (i.e., near-MRC) performance for complexity that matches the actual channel conditions. The authors derive MREC outage probability and average error probability expressions applicable for any correlation. Particular cases apply to BF and MRC. These tools and numerical complexity assessments help demonstrate the advantages of MREC versus BF or MRC in realistic scenarios.

INTRODUCTION

General perspective. Andrew Viterbi is credited with famously stating that "spatial processing remains as the most promising, if not the last frontier, in the evolution of multiple access systems" (Roy, 1998, p. 339). Multiple-antenna-transceiver communications systems, also known as single-input multiple-output (SIMO), multiple-input single-output (MISO), or multiple-input multiple-output (MIMO) systems, which exploit the spatial dimension of the radio channel, promise tremendous benefits over the traditional single-input single-output (SISO) transceiver concept, in terms of data rate, subscriber capacity, cell coverage, link quality, transmit power, etc. Such benefits can be achieved with **smart antenna**s, i.e., SIMO, MISO, and MIMO systems that combine baseband signals for optimum performance (Paulraj, Nabar, & Gore, 2005).

Herein, we consider receive smart antennas (i.e., the SIMO case) deployed in noise-limited scenarios with frequency-flat multipath fading (El Zooghby, 2005, Section 3.3) (Jakes, 1974) (Vaughan & Andersen, 2003, Chapter 3), for which the following signal combining techniques have conventionally been proposed:

- ***Statistical beamforming (BF)***, i.e., digitally steering a radio beam along the dominant eigenvector of the correlation matrix of the channel fading gain vector (S. Choi, Choi, Im, & Choi, 2002) (El Zooghby, 2005, Eqn. (5.23), p. 126, Eqns. (5.78–80), p. 148) (Vaughan & Andersen, 2003, Section 9.2.2). BF enhances vs. SISO the *average*, over the fading and noise, signal-to-noise ratio (SNR) by an *array gain* factor that is ultimately proportional to the antenna correlation and is no greater than the number of antenna elements. Since BF requires the estimation of only the projection of the channel gain vector onto the eigenvector mentioned above, it has low numerical complexity. However, BF is effective only for highly-correlated channel gains, i.e., when the intended signal arrives with narrow azimuth angle spread (AS).
- ***Maximal-ratio combining (MRC)***, i.e., maximizing the output SNR *conditioned* on the fading gains (Brennan, 2003; Simon & Alouini, 2000). This SNR is computed by averaging over the noise only, i.e., conditioning on the channel gains. When the intended-signal AS is large enough to significantly reduce antenna correlation, MRC can greatly outperform BF as a result of *diversity gain* and array gain, at the cost of much higher numerical complexity incurred due to channel estimation for each antenna element.

Note that, for fully correlated (i.e., coherent) channel gains, both BF and MRC reduce to the classical notion of "beamforming" whereby a beam is formed towards the intended signal arriving from a discrete direction (Monzingo & Miller, 1980; Trees, 2002; Godara, 2004).

Statistical beamforming and diversity combining principles have traditionally been classified, studied, and applied separately, leading to disparate and limited performance analyses of BF and MRC. Furthermore, since BF and MRC optimize the average SNR and the conditioned SNR, respectively, they have opposing performance-maximizing spatial correlation requirements, as well as significantly different, correlation-independent, numerical complexities (Siriteanu, Blostein, & Millar, 2006; Siriteanu, 2006; Siriteanu & Blostein, 2007). Because correlation varies in practice due to variable AS (Algans, Pedersen, & Mogensen, 2002), BF or MRC performance fluctuates, whereas numerical complexity remains constant. Therefore, MRC can actually waste processing resources and power, whereas BF can often perform poorly (Siriteanu *et al.*, 2006; Siriteanu, 2006; Siriteanu & Blostein, 2007).

Limitations of stand-alone BF or MRC deployments can be overcome by jointly exploiting their principles, under the unifying framework of *eigencombining*. ***Maximal-ratio eigencombining (MREC)*** first applies the Karhunen-Loeve Transform (KLT) with several dominant eigenvectors of the channel correlation matrix to recast the received signal vector in a reduced-dimension space, and then optimally combines the new, uncorrelated, signals (Alouini, Scaglione, & Giannakis, 2000; Brunner, Utschick, & Nossek, 2001; F. A. Dietrich & Utschick, 2003; Jelitto & Fettweis, 2002; Siriteanu & Blostein, 2007). The number of eigenvectors used for the KLT is referred to as the MREC order. Minimum and maximum orders render MREC equivalent with BF and MRC, respectively (Alouini *et al.*, 2000; Dong & Beaulieu, 2002; Siriteanu & Blostein, 2007). The KLT decorrelating effect simplifies the performance analysis for MREC, i.e., also for BF and MRC, over the entire correlation range (Alouini *et al.*, 2000; Dong & Beaulieu, 2002; Siriteanu & Blostein, 2007). Eigengain decorrelation also simplifies fading factor estimation and combining implementation over MRC, thus reducing the numerical complexity (Alouini *et al.*, 2000; Siriteanu & Blostein, 2007). For the medium-to-high correlation values (i.e., 0.5 – 0.9) often incurred at base-stations in typical urban scenarios (Siriteanu & Blostein, 2007), MREC can reduce problem dimension vs. MRC, further reducing numerical complexity, while offering near-optimum performance, and thus outperforming BF. Consequently, MREC of order selected to suit the channel and noise statistics or the system load can improve signal processing efficiency over BF and MRC (Siriteanu *et al.*, 2006; Siriteanu, 2006; Siriteanu & Blostein, 2007).

Chapter outline and objectives. The next subsection provides more background information on BF, MRC, and MREC. Then, a signal model is described that incorporates additive noise as well as spatial fading caused by signal arrival with AS, for a base station in typical urban scenarios. The traditional SISO approach is then described, and expressions for symbol-detection performance measures such as the outage probability (OP) and average error probability (AEP) are derived. The conventional antenna array signal processing concepts of BF and MRC are studied afterward, for ideal and adverse fading correlation conditions, and their numerical complexities are compared for actual implementations, which require channel estimation. Next, the BF and MRC principles are unified under the framework of MREC, which is shown to simplify the MRC analysis for channel correlation conditions that render difficult direct MRC study. AEP and OP expressions that are derived for MREC but also cover SISO, BF, and MRC, as well as numerical complexity evaluations, serve to demonstrate the benefits of adaptive-eigencombining-based smarter antennas for realistic scenarios with random AS.

FURTHER BACKGROUND, MOTIVATION, AND LITERATURE REVIEW

SIMO, MISO, and MIMO smart antennas deploying diversity combining, statistical beamforming, space-time coding, and spatial multiplexing can provide tremendous performance and capacity improvements over SISO (S. Choi *et al.*, 2002; El Zooghby, 2005; Goldberg & Fonollosa, 1998; Paulraj *et al.*, 2005; Rooyen, Lotter, & Wyk, 2000; Simon & Alouini, 2000; Stridh, Bengtsson, & Ottersten, 2006; Tse & Viswanath, 2005). However, these multi-antenna algorithms require powerful and, thus, power-hungry baseband processing, and their performance is highly dependent on spatial correlation, which is affected by radio propagation conditions (Salz & Winters, 1994). Nonetheless, latest drafts of standards for wireless communications systems specify multi-antenna transceivers for cellular systems, e.g., 3GPP and 3GPP2, and for area networks, e.g., IEEE802.11n and IEEE802.16e (Hottinen, Kuusela, Hugl, Zhang, & Raghothaman, 2006). In this chapter, we concentrate on improving the performance and efficiency of baseband signal processing for receive smart antennas by jointly exploiting the principles of statistical beamforming (S. Choi *et al.*, 2002; El Zooghby, 2005; Goldberg & Fonollosa, 1998; Rooyen *et al.*, 2000; Stridh, Bengtsson, & Ottersten, 2006) and diversity combining (Brennan, 2003; Simon & Alouini, 2000).

The concept of beamforming originates in the radar literature (Applebaum, 1976), where the intended signal was assumed to arrive from a unique direction, i.e., coherently, without spatial fading (Salz & Winters, 1994). Signals picked up by the receiving antenna array can then be processed optimally with a combiner obtained from the deterministic *array steering vector* (El Zooghby, 2005, Section 5.1.4) (Godara, 2004, Section 2.1.1) (Goldberg & Fonollosa, Section 4.1), to form antenna pattern beams that effectively enhance the intended signal, and thus yield array gain (Godara, 2004, Section 2.2.4). Nevertheless, in practice, signals arrive at the base station with nonzero AS (Algans *et al.*, 2002; 3GPP, 2003; Pedersen, Mogensen, & Fleury, 2000; Vaughan & Andersen, 2003), which produces spatial fading, i.e., loss of coherence between the channel gains at the various antenna elements (Salz & Winters, 1994). Spatial fading can yield diversity gain through maximal-ratio combining (MRC), which maximizes the SNR conditioned on the fading, by projecting the received signal vector onto an estimate of the channel gain vector (Brennan, 2003; Jakes, 1974; Lee, 1982; Simon & Alouini, 2000). However, fading estimation based on pilot-symbol-aided modulation (PSAM) at the transmitter and interpolation at the receiver (Siriteanu & Blostein, 2004; Siriteanu *et al.*, 2006; Siriteanu, 2006) can demand significant processing resources in the case of MRC (Siriteanu *et al.*, 2006; Siriteanu, 2006; Siriteanu & Blostein, 2007). Though less complex than MRC, statistical beamforming (BF), which projects the received signal vector onto the dominant eigenvector of the spatial fading correlation matrix, only maximizes the *average* SNR and therefore is effective only in high-correlation environments (S. Choi *et al.*, 2002, Section III.A) (El Zooghby, 2005, Section 5.3.3) (Goldberg & Fonollosa, 1998, Section 5) (Rooyen *et al.*, 2000, Chapters 5,6) (Stridh, Bengtsson, & Ottersten, 2006, Section III.A) (Vaughan & Andersen, 2003, Section 9.2.2).

Since statistical beamforming and diversity combining have traditionally been addressed separately, joint BF and MRC studies and performance comparisons are few and incomplete (El Zooghby, 2005, Sections 7.6–7) (Hottinen, Tirkkonen, & Wichman, 2003, Section 2.2) (Rooyen *et al.*, 2000, Section 6.4) (Vaughan & Andersen, 2003, Section 9.2.2,9.3.4). Furthermore, existing studies of BF provide incomplete evaluations of the effect on performance of noncoherent channel gains (S. Choi *et al.*, 2002; J. Choi & Choi, 2003) (El Zooghby, 2005, Sections 6.3, 7.6–7) (Rooyen *et al.*, 2000, Sec- tion 5.1.4) (Vaughan & Andersen, 2003, Section 9.2.2). For MRC, on the other hand, performance studies are available even for correlated channel gains, but they do not cover the entire correlation range continuously (Brennan, 2003, Section 8) (F. A. Dietrich & Utschick, 2003) (Jakes, 1974) (Lee, 1982, Section 10.6) (Simon & Alouini, 2000, Section 9.6).

The low complexity of BF and its ability to produce significant array gain for narrow AS have made this algorithm the preferred choice for high spatial correlation scenarios (El Zooghby, 2005, Sections 5.1.4, 5.3.3). Otherwise, the much more complex MRC has been deployed, to yield array and diversity gains. Thus, unfavorable actual correlation results in poor BF and MRC performance (Brennan, 2003, Section VIII) (El Zooghby, 2005, Sections 5.1.1, 9.2) (Rooyen *et al.*, 2000, Sections 6.1.2, 6.2.1, 6.4) (Simon & Alouini, 2000, Section 9.6) (Vaughan & Andersen, 2003, Sections 9.2.2.1–2). The correlation between channel gains at different antenna elements is affected by propagation conditions, i.e., power azimuth spectrum (p.a.s.) type and AS, as well as by antenna geometry (Algans *et al.*, 2002; El Zooghby, 2005; Salz & Winters, 1994; Vaughan & Andersen, 2003). Therefore, unfavorable AS or inadequate interelement distance can drastically reduce or completely eliminate the performance gains achievable in theory with BF and MRC over SISO. As already mentioned, actual deployment of MRC consumes significant processing resources on estimating the individual channel gain factors (Siriteanu *et al.*, 2006; Siriteanu, 2006; Siriteanu & Blostein, 2007) (Vaughan & Andersen, 2003, Section 9.2.1.3), whereas BF requires the estimation of a single fading coefficient (S. Choi *et al.*, 2002, Section III) (Goldberg & Fonollosa,1998, Section 5) (Stridh, Bengtsson, & Ottersten, 2006, Section 2) (Siriteanu *et al.*, 2006; Siriteanu & Blostein, 2007) (Vaughan & Andersen, 2003, Section 9.2.1.3). Furthermore, since in practice the AS fluctuates — slowly,

compared to the channel fading (Algans *et al.*, 2002) (Brunner *et al.*, 2001, Section I) (Alouini *et al.*, 2000, Section 3.3) (Siriteanu & Blostein, 2007, Section II) — the performance of BF or MRC varies, while numerical computational complexity remains constant (Siriteanu *et al.*, 2006; Siriteanu, 2006; Siriteanu & Blostein, 2007).

These disadvantages of conventional receive smart antennas have enticed researchers to devise the more cost-effective approach herein entitled "eigencombining", though also known in the literature as "principal components combining" (Alouini *et al.*, 2000) or as "eigenbeamforming" (Brunner *et al.*, 2001). Unlike in MRC, where the antenna signals are directly combined, eigencombining processes signals obtained by projecting the received signals onto dominant eigenvectors of the channel gain correlation matrix.

Eigencombining has recently been proposed for antenna array receivers as a more versatile technique whose performance and computational requirements can follow the channel statistics (Brunner *et al.*, 2001; J. Choi & Choi, 2003; Jelitto & Fettweis, 2002; F. A. Dietrich & Utschick, 2003; Siriteanu *et al.*, 2006; Siriteanu, 2006; Siriteanu & Blostein, 2007). The origins of eigencombining can be traced to beamspace (data-independent) beamforming (Blogh & Hanzo, 2002, Section 3.2.8) (Godara, 2004, Section 2.6) (Trees, 2002, Sections 3.10, 6.9, 7.10), and particularly to principal-component or eigenspace (data-dependent, adaptive) beamforming (Trees, 2002, Sections 6.8, 7.9), which were proposed for antenna array signal-processing dimension reduction. Eigencombining has been promoted for SIMO transceivers as an enhancement to BF for scenarios with non-zero AS, as well as a lower-complexity alternative to MRC for scenarios with non-rich scattering (Alouini *et al.*, 2000; Brunner *et al.*, 2001; J. Choi & Choi, 2003; Jelitto & Fettweis, 2002; F. A. Dietrich & Utschick, 2003; Siriteanu *et al.*, 2006; Siriteanu, 2006; Siriteanu & Blostein, 2007). The statistics of the channel fading vary slowly compared to the Doppler-induced fading (Sampath, Erceg, & Paulraj, 2005, Section 5.B) (Siriteanu & Blostein, 2007, Section II). Therefore, eigendecomposition-updating (Alouini *et al.*, 2000, Section 3.3) (Goldberg & Fonollosa, 1998, Section 7.2) computations inherent to eigencombining can be distributed over long intervals (Brunner *et al.*, 2001, Section I) and do not add significantly to the per-symbol complexity (Siriteanu & Blostein, 2007, Table II), as shown in (Siemens, 2000).

Transmit-side statistical eigenprocessing is better known in MISO systems as eigenbeamforming (Brunner *et al.*, 2001; Rensburg & Friedlander, 2004) and in MIMO systems as either precoding (Bahrami & Le-Ngoc, 2006; Sampath *et al.*, 2005; Vu & Paulraj, 2006) or eigenbeamforming (Hottinen *et al.*, 2003; Zhou & Giannakis, 2003). Eigenbeamforming based on knowledge of the actual channel vector or matrix has also been proposed, in (Hottinen *et al.*, 2003, Section 2.3.2) (Hottinen *et al.*, 2006) (Paulraj *et al.*, 2005, Section 5.4.4) (Tse & Viswanath, 2005, Section 7.1.1). Accompanied by space-time coding, MISO or MIMO *statistical* precoding promises high performance for low complexity and very low receiver-to-transmitter feedback rate (Brunner *et al.*, 2001, Section 4) (Hottinen *et al.*, 2003, Sections 10.2–3) (Rensburg & Friedlander, 2004; Sampath *et al.*, 2005; Vu & Paulraj, 2006; Zhou & Giannakis, 2003). A range of design criteria — e.g., capacity maximization, error probability minimization — have yielded closely-resembling precoding approaches whereby data is sent over dominant eigenvectors of the transmit-side correlation matrix using water-filling techniques (Bahrami & Le-Ngoc, 2006; Sampath *et al.*, 2005; Vu & Paulraj, 2006; Zhou & Giannakis, 2003). Transmit-side statistical eigenprocessing has shown promise for MISO WCDMA systems (Hottinen et al., 2003, Section 10.2-3), and has already been specified for MIMO in the IEEE 802.16e standard (Hottinen *et al.*, 2006).

From a receive-side perspective, this chapter reviews conventional signal combining approaches and places their priciples and analyses under the unifying framework of eigencombining. Expressions applicable for any correlation conditions are then derived for the outage probability and the average error probability of MREC, MRC, and BF, allowing for realistic performance comparisons. The numerical complexities of actual implementations of BF, MRC, and MREC are also compared. It emerges that, besides unifying and simplifying the analyses of BF and MRC, MREC can be adapted to channel and noise statistics for more efficient antenna array signal processing than with stand-alone BF or MRC.

SIGNAL AND CHANNEL MODELS

Received Signal Model

This chapter focuses on receiver-side multibranch signal combining (i.e., SIMO). Although we will present numerical results only for base-station antenna arrays, the subsequent analysis applies for any other multibranch receivers, e.g., subscriber-station antenna arrays or CDMA Rake receivers (El Zooghby, 2005, Section 2.3.3.3) (Patenaude, Lodge, & Chouinard, 1999) (Simon & Alouini, 2000, Section 7.1, p. 160).

Hereafter we assume that L replicas of the transmitted signal are available at the receiver, affected by multipath fading (El Zooghby, 2005; Jakes, 1974; Lee, 1982; Ertel, Cardieri, Sowersby, Rappaport, & Reed, 1998; J. C. Liberti

& Rappaport, 1999; Paulraj *et al.*, 2005; Tse & Viswanath, 2005) and additive noise. These replicas are further referred to as *branches*. After demodulation, matched-filtering, and symbol-rate sampling, the baseband complex-valued received signal vector can be written based on (Proakis, 2001, Eqn. 14.4–1, p. 822) as

$$\tilde{\mathbf{y}} = \sqrt{E_s}\, b\, \tilde{\mathbf{h}} + \tilde{\mathbf{n}}, \tag{1}$$

where b is the M-ary phase-shift-keying (M–PSK) (Simon & Alouini, 2000, Section 3.1.3, p. 35) random, equiprobable, zero-mean, unit-variance transmitted symbol, and E_s is the average energy transmitted per symbol, while $\tilde{\mathbf{h}}$ and $\tilde{\mathbf{n}}$ are the complex-valued, mutually uncorrelated **channel gain** and receiver interference-plus-noise vectors, respectively. The $L \times 1$-dimensional complex-valued vectors from (1) are detailed below:

$$\tilde{\mathbf{y}} = [\tilde{y}_1 \quad \tilde{y}_2 \quad \dots \quad \tilde{y}_L]^T, \quad \tilde{\mathbf{h}} = [\tilde{h}_1 \quad \tilde{h}_2 \quad \dots \quad \tilde{h}_L]^T, \quad \tilde{\mathbf{n}} = [\tilde{n}_1 \quad \tilde{n}_2 \quad \dots \quad \tilde{n}_L]^T. \tag{2}$$

The components of the received signal vector, i.e., the branches, can be written as

$$\tilde{y}_i = \sqrt{E_s}\, b\, \tilde{h}_i + \tilde{n}_i, \quad i = 1 : L \overset{\Delta}{=} 1, \dots, L. \tag{3}$$

The interference-plus-noise vector is assumed to be a zero-mean circularly-symmetric complex-valued Gaussian (ZMC-SCG) (Paulraj *et al.*, 2005, p. 39) spatially- and temporally-white random vector, with variance N_0 per component. For simplicity, we will refer to $\tilde{\mathbf{n}}$ simply as the noise vector. Its distribution is described using the following notation:

$$\tilde{\mathbf{n}} \sim \mathcal{N}_c(\mathbf{0}, N_0 \mathbf{I}). \tag{4}$$

Fading Channel Model

Since we later deal with the impact of spatial fading correlation on multi-antenna array receiver performance, we propose here a simple, relevant, and realistic channel model, based on (3GPP, 2003; Algans *et al.*, 2002; Vaughan & Andersen, 2003). Assume that the transmitted signal reaches the receiver after propagation over Q paths possibly arriving with distinct azimuth angles. Even when there is no azimuth dispersion, several paths could still exist due to scattering over a small area around the subscriber station (Vaughan & Andersen, 2003, Section 9.2.1.2). Assuming that all these paths arrive within the same symbol interval (i.e., flat fading), the channel gain vector can then be written as (El Zooghby, 2005, Eqn. (5.9), p. 123) (Ertel *et al.*, 1998, p. 16)

$$\tilde{\mathbf{h}} = \frac{1}{\sqrt{Q}} \sum_{q=1}^{Q} \alpha_q\, \mathbf{a}(\theta_q), \tag{5}$$

where α_q represents the complex-valued attenuation of the path with angle of arrival (AoA) θ_q with respect to the antenna array broadside (the line perpendicular on the line connecting the array elements), and $\mathbf{a}(\theta_q)$ is the corresponding so-called *array steering vector* (El Zooghby, 2005, Section 5.1.4) (Godara, 2004, Section 2.1.1) (Goldberg & Fonollosa, Section 4.1). For a uniform linear array — ULA (Trees, 2002, Section 2.3) — with normalized interelement distance, i.e., ratio between the physical interelement distance and half of the transmitted-signal carrier wavelength, denoted hereafter as d_n, the array steering vector can be written as (Brunner *et al.*, 2001, p. 4) (Goldberg & Fonollosa, Eqn. (4))

$$\mathbf{a}(\theta_q) = \begin{bmatrix} 1 & e^{-j\pi d_n \sin\theta_q} & \dots & e^{-j\pi(L-1)d_n \sin\theta_q} \end{bmatrix} \tag{6}$$

We follow the Gaussian wide-sense stationary uncorrelated scattering model (Ertel *et al.*, 1998, p. 16). Then, for $Q > 10$, the channel gain vector from (5) is approximately a ZMCSCG vector, i.e.,

$$\tilde{\mathbf{h}} \sim \mathcal{N}_c(\mathbf{0}, \mathbf{R}_{\tilde{\mathbf{h}}}), \tag{7}$$

where

$$\mathbf{R}_{\tilde{\mathbf{h}}} \stackrel{\Delta}{=} E\{\tilde{\mathbf{h}}\tilde{\mathbf{h}}^H\} \tag{8}$$

is the channel gain vector correlation (in this case, also covariance) matrix (Proakis, 2001, p. 33), which is Hermitian. Refer to (Trees, 2002, Appendix A) for the matrix properties invoked herein. Note that ZMCSCG channel gains imply Rayleigh fading (Simon & Alouini, 2000, Section 2.2.1.1).

The numerical results shown throughout this work assume a Toeplitz structure for $\mathbf{R}_{\tilde{\mathbf{h}}}$, i.e., the elements on each left-right diagonal are equal. Then, the first line of $\mathbf{R}_{\tilde{\mathbf{h}}}$ provides the information on all its elements. This applies when the signals are received with a ULA.

The elements on the main diagonal of this matrix, i.e.,

$$\left(\mathbf{R}_{\tilde{\mathbf{h}}}\right)_{i,i} = E\{|\tilde{h}_i|^2\} \stackrel{\Delta}{=} \sigma^2_{\tilde{h}i}, \quad i = 1:L, \tag{9}$$

are the autocorrelations and also the variances (Proakis, 2001, p. 32) of the individual channel gains. They are assumed equal for the numerical results shown in this work. Such assumption is valid for antenna arrays, but not for CDMA Rake receiver taps (Alouini *et al.*, 2000) (Patenaude, Lodge, & Chouinard, 1999). Nonetheless, the subsequent analysis applies for any multibranch receiver.

Using (3), (4), and (9), the signal-to-noise ratio (SNR) for the i th branch given the corresponding channel gain, i.e., the **conditioned SNR** or the symbol-detection SNR, can be written as

$$\tilde{\gamma}_i \stackrel{\Delta}{=} \frac{E_s}{N_0}|\tilde{h}_i|^2, \tag{10}$$

with average over the fading distribution, i.e., **average SNR**, given by

$$\tilde{\Gamma}_i \stackrel{\Delta}{=} \frac{E_s}{N_0}\sigma^2_{\tilde{h}i} = \log_2 M\, \gamma_b\, \sigma^2_{\tilde{h}i}, \tag{11}$$

where $\gamma_b \stackrel{\Delta}{=} \frac{1}{\log_2 M}\frac{E_s}{N_0}$ represents the *average bit-SNR*.

As shown later, propagation conditions (wave scattering) determine antenna correlation, which impacts the performance of antenna array signal processing algorithms. The eigendecomposition of the channel correlation matrix illustrates the distribution of intended-signal power along the eigenvectors of $\mathbf{R}_{\tilde{\mathbf{h}}}$.

Let us discuss a few features of the correlation matrix and its eigendecomposition (Trees, 2002, Appendix A). The Hermitian matrix $\mathbf{R}_{\tilde{\mathbf{h}}}$ has real-valued non-negative eigenvalues, which we consider ordered as

$$\lambda_1 \geq \lambda_2 \geq \ldots \geq \lambda_L \geq 0. \tag{12}$$

The corresponding eigenvectors of $\mathbf{R}_{\tilde{\mathbf{h}}}$, denoted as $\mathbf{u}_i$, i = 1:L, form an orthonormal basis in $\mathbb{C}^L$, i.e., the space of complex-valued L-dimensional vectors. The *eigendecomposition* of $\mathbf{R}_{\tilde{\mathbf{h}}}$ is described by

$$\mathbf{R}_{\tilde{\mathbf{h}}} = \mathbf{U}_L \Lambda_L \mathbf{U}_L^H = \sum_{i=1}^{L} \lambda_i \mathbf{u}_i \mathbf{u}_i^H, \tag{13}$$

where $\mathbf{\Lambda}_L$ is a diagonal matrix having the eigenvalues of $\mathbf{R}_{\tilde{\mathbf{h}}}$ on the main diagonal, and $\mathbf{U}_L \stackrel{\Delta}{=} [\mathbf{u}_1 \quad \mathbf{u}_2 \quad \ldots \quad \mathbf{u}_L]$ is a unitary matrix. The trace of the channel vector correlation matrix, i.e.,

$$tr(\mathbf{R}_{\tilde{\mathbf{h}}}) \stackrel{\Delta}{=} \sum_{i=1}^{L} \left(\mathbf{R}_{\tilde{\mathbf{h}}}\right)_{i,i} = \sum_{i=1}^{L} \sigma_{\tilde{h}_i}^2 = \lambda_1 + \lambda_2 + \ldots + \lambda_L,$$

is a measure of the received intended-signal power. Eigenvectors corresponding to larger eigenvalues are denoted as *dominant*.

The following propositions have simple proofs (not shown here).

Proposition 1 *The elements of the* ***channel gain*** *vector* $\tilde{\mathbf{h}}$ *are coherent – i.e., we can write* $\tilde{\mathbf{h}} = h_1 \mathbf{u}_1$, *where* $h_1 \stackrel{\Delta}{=} \mathbf{u}_1^H \tilde{\mathbf{h}}$ *— if and only if (iff)* $\lambda_1 = tr(\mathbf{R}_{\tilde{\mathbf{h}}})$. In general, two random variables are referred to as coherent or fully correlated if the absolute value of their correlation coefficient is 1.

Proposition 2 *The elements of* $\tilde{\mathbf{h}}$ *are uncorrelated, i.e.,* $(\mathbf{R}_{\tilde{\mathbf{h}}})_{i,j} \stackrel{\Delta}{=} E\{\tilde{h}_i \tilde{h}_j^*\} = \lambda \delta_{i,j}$, *iff the eigenvalues of* $\mathbf{R}_{\tilde{\mathbf{h}}}$ *are all equal, i.e.,*

$$\lambda_i = \lambda = \frac{1}{L} tr(\mathbf{R}_{\tilde{\mathbf{h}}}), \quad i = 1:L.$$ ($\delta_{i,j}$ = 1 for $i = j$, and $\delta_{i,j}$ = 0 for $i \neq j$.)

If the eigenvalues are all equal then $\mathbf{R}_{\tilde{\mathbf{h}}} = \lambda \mathbf{I}$, and we can consider $\mathbf{U}_L = \mathbf{I}_L$.

Power Azimuth Spectrum and Azimuth Angle Spread Models

Definitions. In wireless communications, wave scattering (Ertel *et al.*, 1998; Jakes, 1974; Lee, 1982; Tse & Viswanath, 2005; Vaughan & Andersen, 2003) induces azimuthal angle dispersion, which has been thoroughly characterized in recognition of its important effect on spatial fading correlation and thus on antenna array performance (El Zooghby, 2005, Section 3.8) (Salz & Winters, 1994).

The channel spatial selectivity, i.e., the antenna decorrelation, is affected by the **power azimuth spectrum** (p.a.s.), which is the distribution of received intended-signal power vs. the azimuth angle (Algans *et al.*, 2002, Eqn. (2)) (El Zooghby, 2005, p. 69) (Pedersen, Mogensen, & Fleury, 2000, Eqn. (10)) (Vaughan & Andersen, 2003, Section 4.6), i.e.,

$$P(\theta) = \frac{1}{Q} \sum_{q=1}^{Q} E\{|\alpha_q|^2\} \delta(\theta - \theta_q), \tag{14}$$

for the channel gain vector described by (5). Averaging is over α_q, and $\delta(\cdot)$ represents the Dirac delta function. The square-root second central moment of the p.a.s. is hereafter referred to as ***azimuth spread*** **(AS)** as in (3GPP, 2003, Section 4.6.2) (Algans *et al.*, 2002, p. 525) (El Zooghby, 2005, Eqn. (3.10), p. 71) (Pedersen, Mogensen, & Fleury, 2000, p. 438) (Vaughan & Andersen, 2003, Section 4.6.1).

Power Azimuth Spectrum Model. The Laplacian p.a.s. accurately models actual radio channel measurements for rural, sub/urban, and indoor scenarios (Algans *et al.*, 2002) (Pedersen, Mogensen, & Fleury, 2000) (Vaughan & Andersen, 2003), and was therefore adopted for simulation purposes by wireless systems standardization organizations (3GPP, 2003, Section 4.5.4) (El Zooghby, 2005, p. 70). Based on (3GPP, 2003, Section 4.5.4) (El Zooghby, 2005, Eqn. (3.8), p. 70) (Pedersen, Mogensen, & Fleury, 2000, Eqn. (17)) (Vaughan & Andersen, 2003, Section 4.6.2), we can write a truncated Laplacian p.a.s. as

$$P(\theta) = \begin{cases} \dfrac{1}{1-\exp\left\{-\dfrac{\pi}{\sigma/\sqrt{2}}\right\}} \cdot \dfrac{1}{2\cdot\sigma/\sqrt{2}} \cdot \exp\left\{-\dfrac{|\theta-\theta_c|}{\sigma/\sqrt{2}}\right\} & \text{, for } \theta \in [\theta_c - \pi, \theta_c + \pi], \\ 0 & \text{, otherwise,} \end{cases} \tag{15}$$

where θ_c is the mean AoA, while σ approximates the AS. The numerical results shown in this chapter rely on this p.a.s. model.

For this truncated Laplacian p.a.s., mathematical operations similar to those in (Salz & Winters, 1994, Appendix) produce the following expressions for the real and imaginary parts of the (m, n)th element of $\mathbf{R}_{\tilde{\mathbf{h}}}$ for a ULA:

$$\begin{aligned} \Re\{(\mathbf{R}_{\tilde{\mathbf{h}}})_{m,n}\} &= J_0(z_{m,n}) + 2\sum_{k=1}^{\infty} J_{2k}(z_{m,n}) \frac{\cos(2k\theta_c)}{1+\left[2k\sigma/\sqrt{2}\right]^2} \\ \Im\{(\mathbf{R}_{\tilde{\mathbf{h}}})_{m,n}\} &= \frac{1+\exp\left\{-\dfrac{\pi}{\sigma/\sqrt{2}}\right\}}{1-\exp\left\{-\dfrac{\pi}{\sigma/\sqrt{2}}\right\}} \cdot 2\sum_{k=0}^{\infty} J_{2k+1}(z_{m,n}) \frac{\sin[(2k+1)\theta_c]}{1+\left[(2k+1)\sigma/\sqrt{2}\right]^2}, \end{aligned} \tag{16}$$

where $J_i(\cdot)$ is the ith-order Bessel function of the first kind (Abramowitz & Stegun, 1995, §9.1.21, p. 360), and $z_{m,n} \triangleq \pi(m-n)d_n$. Numerical results shown in this work assume $d_n = 1$ and $\theta_c = 0$; the latter yields real-valued interelement correlation.

Azimuth Spread Distribution Model for Typical Urban Scenarios. Measurements have shown that the AS depends on the environment, antenna array location and height, and is time-varying (Algans *et al.*, 2002). Typical sub/urban base-station AS — measured in degrees — is well modeled by a random variable with lognormal distribution, i.e., (3GPP, 2003; Algans *et al.*, 2002) (El Zooghby, 2005, Eqn. (3.21), p. 75)

$$AS = 10^{\varepsilon x + \mu}; \quad x \sim \mathcal{N}(0,1). \tag{17}$$

For numerical results shown towards the end of the chapter we consider the typical urban scenario measured in (Algans *et al.*, 2002) and described in Table 1, for which $\varepsilon = 0.47$, and $\mu = 0.74$. There, the **azimuth spread** takes predominantly small-to-moderate values, e.g., $Pr(1^\circ < AS < 20^\circ) \approx 0.8$ (3GPP, 2003, Figure 5.6) (Algans *et al.*, 2002, Figure 1).

Besides Doppler-induced temporal channel fading, subscriber station motion also causes AS variations (Algans *et al.*, 2002, Section V) (Vaughan & Andersen, 2003, Section 4.6.1). The expression for the AS correlation over distance (or, equivalently, time) was empirically determined for typical urban scenarios in (Algans *et al.*, 2002) as

$$\rho_{AS}(d) = e^{-d/d_{AS}}, \tag{18}$$

where d is the distance traveled by the subscriber station, and d_{AS} is the AS decorrelation distance, i.e., the distance over which the AS correlation decreases by a factor of three. This distance is typically several orders of magnitude larger than the fading coherence distance (Sampath *et al.*, 2005, p. 407) (Siriteanu & Blostein, 2007, p. 918) (Vu & Paulraj, 2006, p. 2320).

Table 1. Typical urban scenario features

Buildings height/distribution	4-6 floors/uniform density
Street layout	irregular
Line-of-sight	not present
Subscriber station – base station distance	0.2 to 1.1 km
Antenna location/height	above rooftop level/32 m-high

Figure 1. Top: Correlation between adjacent ULA elements, ρ, computed using (16), and the eigenvalues of $\mathbf{R}_{\tilde{\mathbf{h}}}$*, for* d_n = 1, $\theta_c = 0^o$*, and Laplacian power azimuth spectrum. Bottom: Partial sums of eigenvalues, in percentage of* $tr(\mathbf{R}_{\tilde{\mathbf{h}}})$.

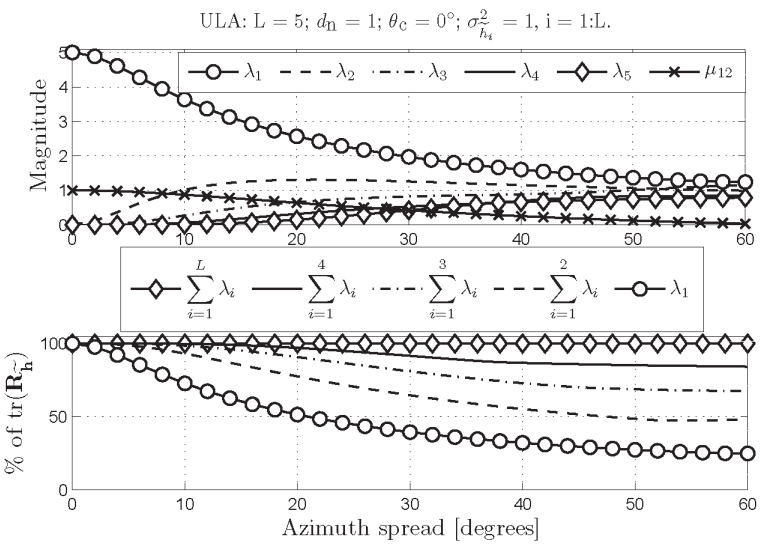

Azimuth Spread Effect on Channel Gain Correlation

We conclude this section on signal and channel models with a numerical illustration. Consider a ULA with L = 5 and d_n = 1, and unit-variance channel gains. Then, for $\theta_c = 0^o$, the top subplot in Figure 1 shows the correlation, ρ, between any two adjacent antennas, computed with (16), and the eigenvalues, $\lambda_i, i = 1:L$, of the channel gain correlation matrix, $\mathbf{R}_{\tilde{\mathbf{h}}}$. On the horizontal axis we represent the AS. The bottom subplot displays the partial eigenvalue sums,

$$\sum_{i=1}^{N}\lambda_i, N = 1:L.$$

For zero AS the channel gains are coherent and $\lambda_1 \neq 0, \lambda_{2:L} = 0$. For low AS, the channel gains are highly correlated and the received intended-signal power, proportional to $tr(\mathbf{R}_{\tilde{\mathbf{h}}})$, is mostly concentrated along a few eigenvectors. Increasing AS yields decreasing antenna correlation, and the intended-signal power is distributed more uniformly along more eigenvectors.

CONVENTIONAL RECEIVERS

In this section we introduce conventional receiver algorithms and study the impact of channel correlation on their performance. The numerical complexity associated with actual implementations of these algorithms is also evaluated.

The Single-Input Single-Output (SISO) Concept

Hereafter we will use the index 0 to indicate SISO variables and performance measures. For SISO, the received signal model is similar to that shown in (3). Assuming perfectly known channel at the receiver, the combiner $w_0 = \tilde{h}_0^*$, i.e., the complex-conjugate of the actual channel gain, maximizes the conditioned SNR, i.e.,

$$\gamma_0 \stackrel{\Delta}{=} \frac{E_s}{N_0} |\tilde{h}_0|^2 . \tag{19}$$

Let us denote with σ_0^2 the variance of the SISO channel gain, i.e., $\sigma_0^2 = E\{|\tilde{h}_0|^2\}$.

For our assumptions of Rayleigh fading, γ_0 can be shown (Simon & Alouini, 2000, p. 18) (Proakis, 2001, p. 44) to have a central chi-square distribution (Proakis, 2001, p. 41) with 2 degrees of freedom, i.e., $\gamma_0 \sim \chi^2(2)$, or, equivalently, an exponential distribution (Simon & Alouini, 2000, p. 20), which is described by the probability density function (p.d.f.)

$$p(\gamma_0) = \begin{cases} 1/\Gamma_0 \exp\left(-\gamma_0/\Gamma_0\right) & \text{,for } \gamma_0 \geq 0, \\ 0 & \text{,otherwise,} \end{cases} \tag{20}$$

where

$$\Gamma_0 \stackrel{\Delta}{=} E\{\gamma_0\} = \frac{E_s}{N_0}\sigma_0^2$$

is the average SNR for the SISO receiver. Then, the variance of γ_0 is given by Γ_0^2 (Proakis, 2001, Eqn. (2.1-12), p. 42). Furthermore, the cumulative distribution function (c.d.f.) of γ_0 is (Jakes, 1974, Eqn. (10-64), p. 310) (Lee, 1982, Eqn. (5.2-15), p. 319)

$$P(\gamma_0) = \begin{cases} 1 - \exp\left(-\gamma_0/\Gamma_0\right) & \text{,for } \gamma_0 \geq 0, \\ 0 & \text{,otherwise,} \end{cases} \tag{21}$$

which measures the probability that the conditioned output SNR is smaller than a threshold, and thus represents an alternate definition of the ***outage probability*** (Simon & Alouini, 2000, p. 5).

Given the conditioned SNR at the output of an optimal combiner, γ_0, the conditioned symbol **error probability** for M–PSK can be written as (Simon & Alouini, 2000, Eqn. 8.22, p. 198)

$$P_e(\gamma_0) = \frac{1}{\pi}\int_0^{\frac{M-1}{M}\pi} \exp\left(-\gamma_0 \frac{g_{PSK}}{\sin^2\phi}\right) d\phi, \tag{22}$$

where

$$g_{PSK} \stackrel{\Delta}{=} \sin^2\frac{\pi}{M}.$$

Note that similar finite-limit integral expressions in exponential functions also describe other modulations (Simon & Alouini, 2000, Chapter 8).

In a fading channel, the conditioned error probability defined in (22) is a random variable, which suggests two different symbol-detection performance measures (Simon & Alouini, 2000, Section 1.1.2, p. 5): 1) the already mentioned

outage probability (OP), actually defined as the probability that the conditioned error rate exceeds a given threshold; 2) the **average error probability (AEP)**, defined as the average over the fading of the conditioned error probability.

The following AEP derivation technique is taken from (Simon & Alouini, 2000, Chapter 9). By definition, the AEP is

$$P_{\mathrm{e}} \stackrel{\Delta}{=} \int_0^{\infty} P_{\mathrm{e}}(\gamma_0)\, p(\gamma_0)\, d\gamma_0 \tag{23}$$

Substituting $P_e(\gamma_0)$ from (22) in (23) yields the AEP expression as

$$P_{\mathrm{e}} = \frac{1}{\pi}\int_0^{\frac{M-1}{M}\pi}\int_0^{\infty} \exp\left(-\gamma_0 \frac{g_{PSK}}{\sin^2\phi}\right) p(\gamma_0)\, d\gamma_0\, d\phi. \tag{24}$$

Since the moment generating function (m.g.f.) of γ_0 is by definition $M_{\gamma_0}(s) \stackrel{\Delta}{=} E\{e^{s\gamma_0}\}$ (Simon & Alouini, 2000, Eqn. 2.4, p. 18), the AEP can be written as

$$P_{\mathrm{e}} = \frac{1}{\pi}\int_0^{\frac{M-1}{M}\pi} M_{\gamma_0}\left(-\frac{g_{PSK}}{\sin^2\phi}\right) d\phi. \tag{25}$$

For our Rayleigh fading assumptions the m.g.f. of γ_0 is given by (Simon & Alouini, 2000, Table 2.2, p. 19)

$$M_{\gamma_0}(s) = (1 - s\Gamma_0)^{-1}. \tag{26}$$

Then, Eqn. (25) yields the following simple finite-limit integral (thus, nonclosed-form) SISO AEP expression for M–PSK:

$$P_{\mathrm{e,SISO}} = \frac{1}{\pi}\int_0^{\frac{M-1}{M}\pi}\left(1 + \Gamma_0 \frac{g_{PSK}}{\sin^2\phi}\right)^{-1} d\phi. \tag{27}$$

Similar results are possible for other modulations, as well as for Ricean and Nakagami-*m* fading (Alouini *et al.*, 2000) (Simon & Alouini, 2000, Table 9.1, p. 269).

Above we have looked at the SISO case. Hereafter, SIMO signal processing algorithms are described and analyzed.

Maximum-Average-SNR (Statistical) Beamforming (BF) and Array Gain

Statistical Beamforming Procedure. The objective of statistical beamforming (BF) is to find a combiner $\tilde{\mathbf{w}}$ for $\tilde{\mathbf{y}}$ in (1) that maximizes the SNR obtained by averaging over fading and noise. After the linear combining

$$\tilde{\mathbf{w}}^H \tilde{\mathbf{y}} = \sqrt{E_s}\, b \tilde{\mathbf{w}}^H \tilde{\mathbf{h}} + \tilde{\mathbf{w}}^H \tilde{\mathbf{n}} \tag{28}$$

the output power, averaging over noise and fading, is

$$E\{|\tilde{\mathbf{w}}^H \tilde{\mathbf{y}}|^2\} = E_s E\{|\tilde{\mathbf{w}}^H \tilde{\mathbf{h}}|^2\} + E\{|\tilde{\mathbf{w}}^H \tilde{\mathbf{n}}|^2\} = E_s \tilde{\mathbf{w}}^H \mathbf{R}_{\tilde{\mathbf{h}}} \tilde{\mathbf{w}} + N_0 \tilde{\mathbf{w}}^H \tilde{\mathbf{w}}, \tag{29}$$

which yields the average output SNR as

$$SNR_{\text{avg}}(\widetilde{\mathbf{w}}) \stackrel{\Delta}{=} \frac{E_s}{N_0} \frac{\widetilde{\mathbf{w}}^H \mathbf{R}_{\tilde{\mathbf{h}}} \widetilde{\mathbf{w}}}{\widetilde{\mathbf{w}}^H \widetilde{\mathbf{w}}}. \tag{30}$$

The second ratio in (30) is a Rayleigh quotient (Golub & Loan, 2000), whose properties yield

$$\frac{E_s}{N_0}\lambda_L \leq SNR_{\text{avg}}(\widetilde{\mathbf{w}}) \leq \frac{E_s}{N_0}\lambda_1. \tag{31}$$

The lower bound is achieved with a combiner proportional to $\mathbf{u}_L$, i.e., $\widetilde{\mathbf{w}} \propto \mathbf{u}_L$. The upper bound is achieved with $\widetilde{\mathbf{w}}_{BF} \propto \mathbf{u}_1$, which therefore represents maximum-average-SNR, or statistical, beamforming (BF). Coherent detection requires

$$\widetilde{\mathbf{w}}_{BF} = h_1 \mathbf{u}_1, \tag{32}$$

where $h_1 \stackrel{\Delta}{=} \mathbf{u}_1^H \tilde{\mathbf{h}}$. Recovery of a BPSK symbol, for instance, is attempted as follows:

$$\hat{b}_{BF} = sign\left\{\Re\left[\widetilde{\mathbf{w}}_{BF}^H \tilde{\mathbf{y}}\right]\right\}. \tag{33}$$

BF Performance Analysis. Array Gain. After substituting (32) into (28) we can write the conditioned output SNR for BF as

$$\gamma_1 \stackrel{\Delta}{=} \frac{E_s}{N_0} |\mathbf{u}_1^H \tilde{\mathbf{h}}|^2 = \frac{E_s}{N_0} |h_1|^2 . \tag{34}$$

It has been demonstrated in (Alouini *et al.*, 2000, Section 4.1) that $h_1 \sim \mathcal{N}_c(0, \lambda_1)$, so that γ_1 is exponentially distributed, with average

$$\Gamma_1 \stackrel{\Delta}{=} E\{\gamma_1\} = \frac{E_s}{N_0}\lambda_1. \tag{35}$$

Thus, the BF conditioned output SNR has the same distribution type as for each of the branches, but with a different average — see the SISO output SNR p.d.f. in (20). The average output SNR is an appropriate performance measure for SISO and BF because it completely describes the p.d.f. of the conditioned output SNR. Communications systems terminology typically denotes as *array gain* (Godara, 2004, Section 2.2.4) (Paulraj *et al.*, 2005, p. 91) (Vaughan & Andersen, 2003, Section 9.2.2) an increase in average SNR due to multibranch combining. The BF **array gain** is then (in decibels)

$$G_{A,BF,dB} = 10\log_{10}\left(\Gamma_1 / \Gamma_0\right). \tag{36}$$

Propositions 1 and 2 indicate that

$$\Gamma_1 = \frac{E_s}{N_0}\lambda_1 \in \left[\frac{E_s}{N_0}\frac{1}{L} tr(\mathbf{R}_{\tilde{\mathbf{h}}}), \frac{E_s}{N_0} tr(\mathbf{R}_{\tilde{\mathbf{h}}})\right], \tag{37}$$

where the lower and upper bounds are achieved for uncorrelated and coherent branches, respectively. For unit-variance channel gains we have $tr(\mathbf{R}_{\tilde{\mathbf{h}}}) = L$, so that

$$G_{A,BF,dB} \in \left[0, 10\log_{10} L\right], \tag{38}$$

i.e., the BF combiner in (32) yields a maximum array gain of $G_{A,BF,dB} = 10\log_{10} L$ for coherent channel gains, and no array gain whatsoever for uncorrelated branches (Vaughan & Andersen, 2003, Sections 9.2.2.1–2, 9.3.4). Therefore, BF should only be employed for low AS.

Figure 2 shows the p.d.f.s of the conditioned SNR for SISO and for a ULA BF antenna with $L = 5$ coherent and unit-variance channel gains. Note that the abscissa is in dB. Compared to SISO, BF yields higher probabilities for large conditioned-SNR values and lower probabilities for small conditioned-SNR values.

Now, the same approach that has lead to the SISO AEP expression from (27), produces for M–PSK and BF the AEP expression

$$P_{\mathrm{e,BF}} = \frac{1}{\pi}\int_0^{\frac{M-1}{M}\pi}\left(1+\Gamma_1\frac{g_{PSK}}{\sin^2\phi}\right)^{-1} d\phi, \tag{39}$$

which applies for any interbranch correlation, i.e., for any AS. Clearly, larger Γ_1 improves BF symbol-detection performance. Propositions 1 and 2, along with (37), confirm that best BF performance is achieved when the channel gains are coherent, i.e., for zero AS. Note also that for $\Gamma_1 = \Gamma_0$, i.e., equal average transmitted power for BF and SISO, or for $L = 1$, the BF AEP expression (39) reduces to the SISO AEP expression from (27).

Figure 3 plots the AEPs, computed with (39), vs. the average bit-SNR, for a BF ULA with $L = 5$ and for SISO, for BPSK and Rayleigh fading, unit-variance, coherent channel gains ($AS = 0$). The left-shift of the BF AEP plot by about 7 dB relative to the SISO AEP plot is due to BF array gain.

Figure 2. The p.d.f. of the conditioned output SNR for SISO — i.e., γ_0 from (19) — and for BF of $L = 5$ coherent branches — i.e., γ_1 from (34) — obtained using (20) accordingly, for $\sigma_0^2 = \sigma_{h_i}^2 = 1,\ \forall i = 1:L$, and average bit-SNR γ_b = 10dB.

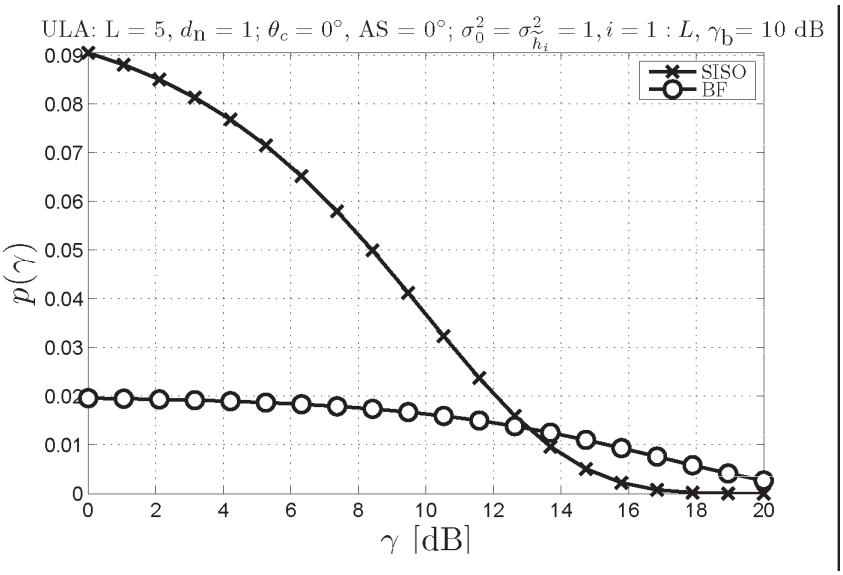

Figure 3. AEP computed with (39) vs. average bit-SNR for BF ULA with L = 5 and for SISO, for BPSK and Rayleigh fading, coherent, unit-variance channel gains.

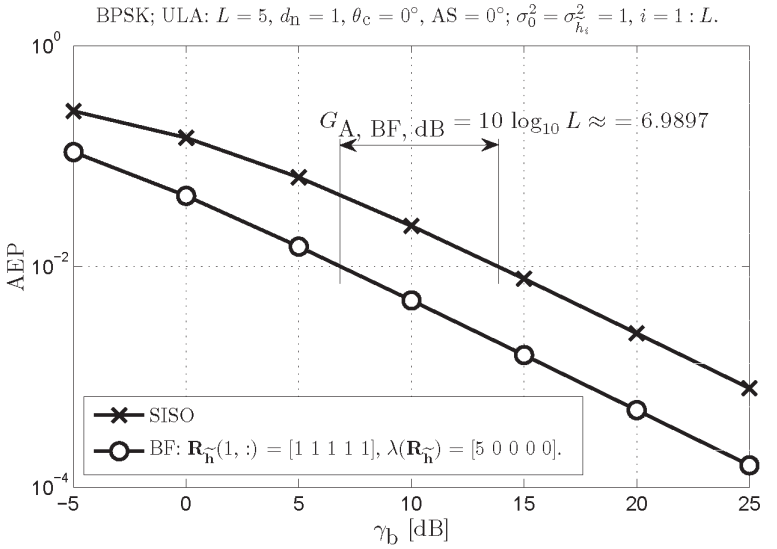

Maximal-Ratio Combining (MRC), Amount of Fading, Diversity Gain, and Diversity Order

While BF originates in the demand to improve reception in line-of-sight links, diversity combining procedures, such as maximal-ratio combining (MRC), were devised precisely with the objective of dealing with the fading caused by rich scattering.

MRC Procedure. Again, the linear combination of the received signal vector described by (1) with a weight vector $\tilde{\mathbf{w}}$ yields

$$\tilde{\mathbf{w}}^H \tilde{\mathbf{y}} = \sqrt{E_s}\, b\, \tilde{\mathbf{w}}^H \tilde{\mathbf{h}} + \tilde{\mathbf{w}}^H \tilde{\mathbf{n}}. \tag{40}$$

The combiner conditioned output power, computed by averaging over the noise distribution, is

$$E\{|\tilde{\mathbf{w}}^H \tilde{\mathbf{y}}|^2\} = E_s |\tilde{\mathbf{w}}^H \tilde{\mathbf{h}}|^2 + E\{|\tilde{\mathbf{w}}^H \tilde{\mathbf{n}}|^2\} = E_s |\tilde{\mathbf{w}}^H \tilde{\mathbf{h}}|^2 + N_0 \tilde{\mathbf{w}}^H \tilde{\mathbf{w}}, \tag{41}$$

so that the conditioned output SNR, i.e., the symbol-detection SNR, is

$$SNR(\tilde{\mathbf{w}}) \stackrel{\Delta}{=} \frac{E_s}{N_0} \frac{|\tilde{\mathbf{w}}^H \tilde{\mathbf{h}}|^2}{\tilde{\mathbf{w}}^H \tilde{\mathbf{w}}}. \tag{42}$$

From the Schwarz inequality (Brennan, 2003, Appendix II) (Lee, 1982, p. 305) we have that

$$\max_{\tilde{\mathbf{w}} \in \mathbb{C}^L} SNR(\tilde{\mathbf{w}}) = SNR(k\, \tilde{\mathbf{h}}) = \frac{E_s}{N_0} |\tilde{\mathbf{h}}|^2 = \sum_{i=1}^{L} \frac{E_s}{N_0} |\tilde{h}_i|^2 . \tag{43}$$

Since the proportionality factor k from (43) does not affect the SNR, the weight vector

$$\tilde{\mathbf{w}}_{MRC} = \tilde{\mathbf{h}} \tag{44}$$

maximizes the combiner-output conditioned-SNR, which is then given by

$$\tilde{\gamma} = \sum_{i=1}^{L} \tilde{\gamma}_i, \tag{45}$$

i.e., the sum of the individual branch SNRs. This justifies the appellative of *maximal-ratio combining* (MRC) for this approach (Brennan, 2003). Maximum-likelihood recovery of a BPSK transmitted symbol, for instance, is attempted as follows:

$$\hat{b}_{MRC} \quad = \quad sign\left\{\Re\left[\tilde{\mathbf{w}}_{MRC}^{H}\ \tilde{\mathbf{y}}\right]\right\} = sign\left\{\Re\left[\tilde{\mathbf{h}}^{H}\ \tilde{\mathbf{y}}\right]\right\}. \tag{46}$$

Averaging in (45) over the fading then yields the **average SNR** for MRC as

$$\tilde{\Gamma} \stackrel{\Delta}{=} E\{\tilde{\gamma}\} = \sum_{i=1}^{L} E\{\tilde{\gamma}_i\} = \sum_{i=1}^{L} \tilde{\Gamma}_i, \tag{47}$$

which, for identically distributed channel gains, indicates that MRC achieves maximum, L-fold, **array gain** over SISO, i.e., $G_{A,MRC,dB} = 10\log_{10} L$ (Vaughan & Andersen, 2003, Section 9.2.2.2, Eqn. 9.2.17). Note that, unlike BF, MRC achieves this maximum array gain regardless of the channel gain correlations. This is because, unlike in BF, the MRC weights are (coherent with) the corresponding channel gains, irrespective of the correlation between channel gains. Nevertheless, the correlation between the channel gains does impact other symbol-detection performance measures for MRC, as will be shown further below.

MRC Performance Analysis for Uncorrelated and Identically Distributed Channel Gains. For the sake of simplicity, many previous MRC analyses have assumed, as we do below, that the Gaussian channel gains are uncorrelated, i.e., independent. For now they are also assumed identically distributed, which implies that all branches have the same average SNR, i.e., $\tilde{\Gamma}_i = \tilde{\Gamma}_1,\ \forall i = 1:L$. Then, it can be shown (Proakis, 2001, Eqn. (2.1-110), p. 41) that the conditioned SNR at the MRC output, i.e., $\tilde{\gamma}$ from (45), has a chi-square distribution with $2L$ degrees of freedom, i.e., $\tilde{\gamma} \sim \chi^2(2L)$, or, equivalently, a Gamma distribution, described by the p.d.f. (Jakes, 1974, Eqn. (5.2-14), p. 319) (Lee, 1982, Eqn. (10-61), p. 310)

$$p(\tilde{\gamma}) = \begin{cases} \dfrac{1}{(L-1)!\,\tilde{\Gamma}_1} \left(\tilde{\gamma}/\tilde{\Gamma}_1\right)^{L-1} \exp\left(-\tilde{\gamma}/\tilde{\Gamma}_1\right) & ,\text{for } \tilde{\gamma} \geq 0, \\ 0 & ,\text{otherwise,} \end{cases} \tag{48}$$

or by the c.d.f. (Jakes, 1974, Eqn. (5.2-15), p. 319) (Lee, 1982, Eqn. (10-64), p. 310)

$$P\left(\tilde{\gamma}\right) = \begin{cases} 1 - \exp\left(-\tilde{\gamma}/\tilde{\Gamma}_1\right) \sum_{l=1}^{L} \dfrac{1}{(l-1)!} \left(\tilde{\gamma}/\tilde{\Gamma}_1\right)^{l-1} & ,\text{for } \tilde{\gamma} \geq 0, \\ 0 & ,\text{otherwise.} \end{cases} \tag{49}$$

Evaluating Diversity Combining Performance: Deep-Fade Probability, Amount of Fading. Receiver performance is determined by the probability of a deep fade, i.e., the probability of subunitary conditioned output SNR value given a high $\tilde{\Gamma}_1$ value (Tse & Viswanath, 2005, p. 55). The above c.d.f. indicates that $Pr(\tilde{\gamma} \leq 0\,dB \,|\, \tilde{\Gamma}_1 = 30\,dB)$ is 10^{-3} for SISO (equivalent to MRC with $L = 1$), $10^{-6.3}$ for MRC of $L = 2$ branches, and only $10^{-9.8}$ for MRC of $L = 3$ branches. Although MRC yields full array gain, this performance improvement is largely due to fading severity reduction, which is explained next.

Fading severity is quantifiable analytically independently of $\widetilde{\Gamma}_1$ and the threshold SNR by the ***amount of fading* (AF)**, which, for a generic combiner with conditioned output SNR denoted as $\tilde{\gamma}$, is given by (Simon & Alouini, 2000, Eqn. 2.5, p. 18)

$$AF \overset{\Delta}{=} \frac{\operatorname{var}\left(\tilde{\gamma}\right)}{\left(E\{\tilde{\gamma}\}\right)^2} = \frac{E\{\tilde{\gamma}^2\} - \left(E\{\tilde{\gamma}\}\right)^2}{\left(E\{\tilde{\gamma}\}\right)^2}. \tag{50}$$

The Rayleigh SISO case yields $AF_{SISO} = 1$. On the other hand, using (47) and (Proakis, 2001, Eqn. (2.1-12), p. 42) it can be shown that, for MRC of L branches with independent and identically distributed (i.i.d.) Rayleigh fading channel gains,

$$AF_{MRC} = \frac{1}{L} \tag{51}$$

i.e., MRC reduces fading severity L-fold.

When comparing combining methods employing a different number of branches, such as MRC and SISO, the variance of the output SNR will capture solely the fading-reducing effect of diversity combining if we require that the combining methods yield the same average output SNR (Proakis, 2001, Eqn. (14.4-34), p. 829). As mentioned earlier, for Rayleigh fading, given the SISO average SNR Γ_0, the variance of the SISO conditioned SNR is Γ_0^2. If for MRC with i.i.d. channel gains we set $\widetilde{\Gamma}_i = \Gamma_0/L,\ \forall i = 1:L$ — so that $\Gamma_0 = \sum_{i=1}^{L} \widetilde{\Gamma}_i$ — then the variance of the MRC conditioned output SNR can be shown to be Γ_0^2 / L, which indicates an L-fold fading severity reduction over SISO.

For this situation, Figure 4 shows the p.d.f. of the conditioned output SNR, computed with (48), for SISO and for MRC with L = 5,9,13,17 i.i.d. branches, given the average output SNR value $\Gamma_0 = \sum_{i=1}^{L} \widetilde{\Gamma}_i$dB. The peak of the p.d.f. increases with L, whereas the standard deviation decreases, i.e., fading severity diminishes. Figure 4 suggests that

$$\lim_{L\to\infty} p(\tilde{\gamma}) = \begin{cases} 1 & \text{, for } \tilde{\gamma} = \Gamma_0, \\ 0 & \text{, otherwise,} \end{cases} \tag{52}$$

which describes the symbol-detection SNR for a SISO nonfading channel.

MRC Performance Analysis for Uncorrelated and Nonidentically Distributed Channel Gains. Let us now derive the MRC AEP for the more encompassing case of uncorrelated channel gains with possibly unequal variances. Using (45) along with the channel gain independence property, the m.g.f. of the conditioned output SNR for MRC can be written as (Simon & Alouini, 2000, Eqn. (9.11), p. 269)

$$M_{\tilde{\gamma}}(s) = \prod_{i=1}^{L} M_{\tilde{\gamma}_i}(s) = \prod_{i=1}^{L} \left(1 - s\tilde{\gamma}_i\right)^{-1}. \tag{53}$$

The AEP derivation procedure used earlier for SISO yields in this case the following AEP expression (Simon & Alouini, 2000, Section 9.2.3.2)

$$P_{\text{e,MRC,indep.}} = \frac{1}{\pi} \int_0^{\frac{M-1}{M}\pi} \prod_{i=1}^{L} \left(1 + \widetilde{\Gamma}_i \frac{g_{PSK}}{\sin^2\phi}\right)^{-1} d\phi. \tag{54}$$

For MRC of i.i.d. channel gains, i.e., when $\sigma_{\tilde{h}_i}^2 = \sigma_{\tilde{h}_1}^2,\ \forall i = 1:L$, the above becomes

$$P_{\text{e,MRC,i.i.d.}} = \frac{1}{\pi} \int_0^{\frac{M-1}{M}\pi} \left(1 + \widetilde{\Gamma}_1 \frac{g_{PSK}}{\sin^2\phi}\right)^{-L} d\phi. \tag{55}$$

Figure 4. The p.d.f. of the conditioned output SNR for SISO and for MRC of L = 5,9,13,17 i.i.d branches, with equal output average SNR, $\Gamma_0 = \sum_{i=1}^{L} \widetilde{\Gamma}_i = 10$ *dB.*

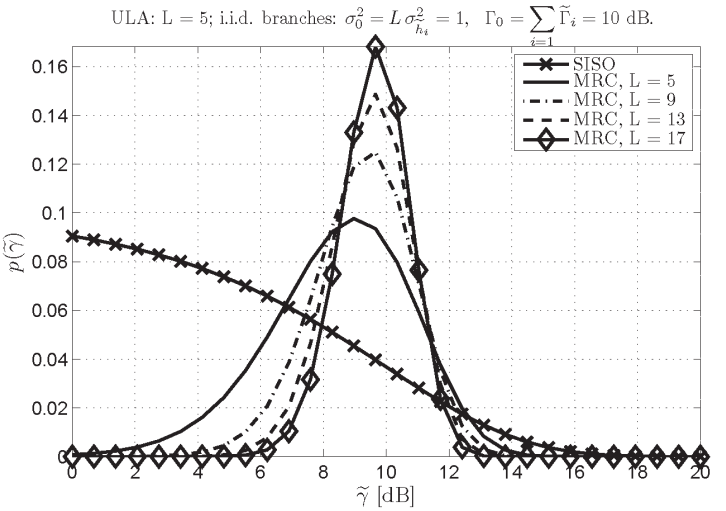

Diversity gain. For BPSK transmitted signal and MRC of L = 1:5 i.i.d. branches with $\sigma_{\tilde{h}_i}^2 = 1$, $i = 1 : L$, Figure 5 displays the AEP computed using (55), vs. the average bit-SNR. For $AEP = 10^{-2}$, MRC with $L = 5$ outperforms SISO by about 15 dB. Of this, about 7 dB is array gain due to coherent combining, i.e., $G_{A,MRC,dB} = 10\log_{10} L$. The remaining 8 dB gain is due to fading severity reduction, and is called ***diversity gain*** (Paulraj *et al.*, 2005, Section 5.2, p. 86). Note that the diversity gain increases with lower AEP and with increasing L. Nevertheless, the diversity gain gradient diminishes as the number of branches increases. This phenomenon and the cost associated with a diversity branch will in practice limit the feasible number of antenna elements.

Diversity order. For BPSK and independent unit-variance Rayleigh fading channel gains, the MRC AEP expression from (55) can be approximated at high average bit-SNR as (Siriteanu & Blostein, 2004, Eqn. (12))

$$P_{\text{e,MRC,i.i.d.}} \approx \frac{(2L)!}{2^{2L+1}(L!)^2}\left(\frac{E_s}{N_0}\right)^{-L}. \tag{56}$$

The SNR exponent in such asymptotic AEP expressions, i.e., the high-SNR AEP curve slope, is commonly referred to as *diversity order* (Paulraj *et al.*, 2005, Section 5.2) (Vaughan & Andersen, 2003, Section 9.3.4). Thus, (56) indicates that MRC has diversity order equal to the number of i.i.d. combined branches. Since

$$10\log_{10} P_{\text{e,MRC,i.i.d.}} \propto -L\left[\frac{E_s}{N_0}\right]_{\text{in dB}}, \tag{57}$$

a 10 dB SNR increase will decrease the AEP by a factor of 10^L at high SNR, which is confirmed by Figure 5.

On the other hand, for a given value of $tr(\mathbf{R}_{\tilde{\mathbf{h}}})$, manipulation of (55) yields

$$\lim_{L\to\infty} P_{\text{e,MRC,i.i.d.}} = \frac{1}{\pi}\int_0^{\frac{M-1}{M}\pi} \exp\left\{-\frac{E_s}{N_0} tr\left(\mathbf{R}_{\tilde{\mathbf{h}}}\right)\frac{g_{PSK}}{\sin^2\phi}\right\} d\phi, \tag{58}$$

which, based on (22), is the error probability for a SISO nonfading channel with SNR equal to

$$\frac{E_s}{N_0} tr\left(\mathbf{R}_{\tilde{\mathbf{h}}}\right).$$

Thus, diversity combining transforms a SIMO fading channel into an equivalent SISO nonfading channel.

The expressions derived above apply for uncorrelated channel gains only. For correlated gains, MRC performance measure expressions are difficult to obtain unless the analysis is tackled from the eigencombining perspective (Alouini *et al.*, 2000; Dong & Beaulieu, 2002; Siriteanu & Blostein, 2007), as described later. Therefore, for the numerical results depicted hereafter for MRC we have actually used the eigencombining AEP expression (82).

Realistic BF and MRC Performance

Above, we have evaluated BF and MRC for perfectly known channel as well as only for their respective performance-maximizing correlation conditions. However, due to changing azimuth spread (AS), actual scenarios can feature variable and possibly unfavorable spatial correlation, impacting the BF and MRC performance as described next. The effect of channel estimation on BF and MRC numerical complexity is discussed further below.

For QPSK, channel gains with unit variance, average bit-SNR $\gamma_b = 5$ dB, ULA, $L = 3$, $d_n = 1$, and $\theta_c = 0$, Figure 6 shows vs. AS the following:

- **Top:** the AEPs for SISO, BF, and MRC, from (27), (39), and (82), respectively.
- **Bottom:** the correlations between adjacent and nonadjacent ULA elements, denoted as $\rho_{1,2}$ and $\rho_{1,3}$, respectively; the eigenvalues $\lambda_i, i = 1 : L$, of the channel correlation matrix $\mathbf{R}_{\tilde{\mathbf{h}}}$.

Note that BF performance is degrading with increasing AS because this decreases the correlation between channel gains, which distributes intended-signal power along an increasing number of eigenvectors of $\mathbf{R}_{\tilde{\mathbf{h}}}$. Thus, the correlation decreases between the applied BF weights from (32) and the channel gains from (3), which reduces the BF array gain. For adjacent channel gain correlation lower than 0.9, BF can be greatly outperformed by MRC. At very high AS, BF yields SISO-like performance. On the other hand, MRC performance improves with increasing AS because the diversity gain increases with decreasing correlation between the channel gains. MRC nears its best performance for adjacent element correlation lower than about 0.5, which is achieved for $AS > 25^\circ$ in this case of $\lambda_c / 2$-spaced antenna elements. Recall that in typical urban scenarios the AS is random with $Pr(1^\circ < AS < 20^\circ) \approx 0.8$. Thus, although MRC may significantly outperform BF, it only seldom achieves maximum diversity gain.

Figure 5. SISO and MRC AEP for BPSK transmitted signal and Rayleigh i.i.d. unit-variance channel gains; the high-SNR slope reveals the diversity order

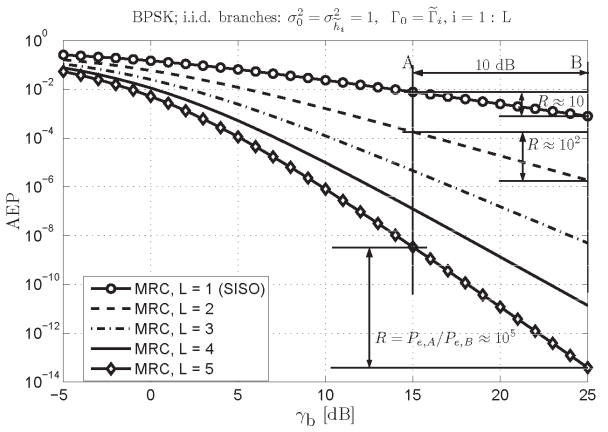

Realistic BF and MRC Numerical Complexity

Let us now discuss our assumptions about the channel knowledge at the receiver, and the numerical complexity incurred to obtain this knowledge and to implement statistical beamforming (BF) and maximal-ratio combining (MRC). The factors affecting the spatial correlation typically change much more slowly than the Doppler-shift-induced temporal fading—see the earlier discussion on azimuth spread temporal correlation. Then, a sufficient number of uncorrelated (Goldberg & Fonollosa, 1998, Section 7.2) samples of the received signal vector are available for accurate channel eigendecomposition updating (Alouini, Scaglione, & Giannakis, 2000, Eqn. (15)) (Brunner *et al.*, 2001, Sections 4.2, 4.3) (Goldberg & Fonollosa, 1998, Eqn. (28)) (Vu & Paulraj, 2006). Therefore, throughout this chapter we assume perfectly known spatial fading eigendecomposition described by (13). Note further that the updating operations can be distributed over long intervals and thus do not significantly increase the per-symbol computational volume (Siemens, 2000).

Although the symbol-detection performance is analyzed for perfectly known channel gains in this chapter, similar procedures readily extend to optimum combining implementation given channel gain estimates and statistical knowledge about the fading and noise, as shown in (Siriteanu & Blostein, 2007, Section III.D). The effect of channel estimation on the performance of a suboptimal, but more practical, implementation, which disregards fading and noise statistics in combiner weight computation, is analyzed in (Siriteanu & Blostein, 2004) (Siriteanu & Blostein, 2007, Appendix). These references contain comprehensive information on the performance of BF and MRC for estimated channel and optimum and suboptimum implementation. Below we evaluate only the numerical complexity incurred by channel estimation and combining implementation in BF and MRC.

Actual implementation of MRC requires the estimation of $\tilde{h}_i$, $i = 1{:}L$, whereas BF only requires the estimation of h_1 if $\mathbf{u}_1$ is perfectly known. These time-varying factors are typically estimated using pilot-symbol-aided modulation (PSAM) at the transmitter and pilot-sample interpolation at the receiver. Pilot symbols are embedded in each slot of the transmitted stream. At the receiver, T pilot samples closest to the symbol for which the fading gain is estimated are used for interpolation. Considered herein are the following typical interpolators: 1) a simple but suboptimal filter whose time-response approaches the sampling function, i.e., $sinc(x) = \sin(\pi x) / (\pi x)$; the estimation method employing this interpolation vector is hereafter denoted as SINC PSAM; 2) the more complex but optimal minimum mean-squared-error approach; the estimation method employing this interpolation method is hereafter denoted as MMSE PSAM. Detailed descriptions of SINC and MMSE PSAM appear in (Siriteanu & Blostein, 2004, Section III.B) (Siriteanu *et al.*, 2006, Section 2.6) (Siriteanu, 2006, Sections 2.5, 3.6).

Figure 6. Top: AEP performance for QPSK, unit-variance channel gains, and average bit-SNR γ_b = 5 dB, for SISO and for BF and MRC ULA with L = 3; Bottom: Correlations between the channel gains corresponding to adjacent and extreme antenna elements, and the eigenvalues of $\mathbf{R}_{\tilde{\mathbf{h}}}$.

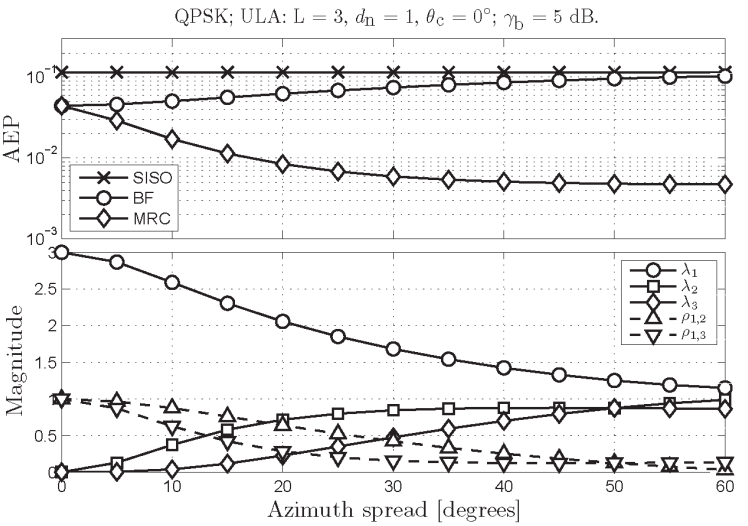

Table 2 reproduces from (Siriteanu & Blostein, 2007, Table II) the numerical complexities of BF and MRC in terms of the number of complex multiplications and additions required per detected symbol for SINC and MMSE PSAM channel estimation and optimum or suboptimum combining implementations. Unlike the performance, the **numerical complexity** of MRC and BF is independent of correlation conditions. The right-most column in Table 2, which displays the MRC-vs.-BF complexity ratio for $L = 4$ and $T = 11$, indicates that MRC can be much more complex than BF. For instance, for SINC PSAM and suboptimum combining, MRC is 3 times more complex than BF. For the same settings, comparisons shown in (Siriteanu *et al.*, 2006) revealed that a field-programmable gate array (FPGA) chip programmed with a fixed-point MRC design consumes about 3 times more dynamic power than its BF counterpart. On the other hand, MRC is more than 11 times more complex than BF for MMSE PSAM because this approach requires joint estimation of all the channel gains using matrix operations (Siriteanu, 2006, Section 3.6.2). For SINC PSAM the channel gains are estimated separately, using only vector inner products (Siriteanu & Blostein, 2004, Eqn. (42)) (Siriteanu, 2006, Eqn. (3.110), p. 83).

The above performance and complexity comparisons indicate that BF and MRC should only be deployed for high (> 0.9) and low (< 0.5) correlation values, respectively. However, as mentioned earlier, actual values predominantly fall between these extremes and are slowly time-varying. Required then is a more flexible approach, hereafter entitled *eigencombining*, that jointly exploits BF and MRC principles, as described next (Siemens, 2000; Alouini *et al.*, 2000; Brunner *et al.*, 2001; J. Choi & Choi, 2003; F. A. Dietrich & Utschick, 2003; Hottinen *et al.*, 2003; Jelitto & Fettweis, 2002; Siriteanu & Blostein, 2007).

MAXIMAL-RATIO EIGENCOMBINING (MREC): SUPERSET OF BF AND MRC

Maximal-ratio eigencombining (MREC) of order N, $1 \le N \le L$, denoted hereafter with MREC_N, consists of two steps:

- The $L \times N$, full column rank, matrix $\mathbf{U}_N \overset{\Delta}{=} [\mathbf{u}_1 \quad \mathbf{u}_2 \quad \dots \quad \mathbf{u}_N]$ comprising the N dominant eigenvectors of $\mathbf{R}_{\tilde{\mathbf{h}}}$ transforms the received signal vector $\tilde{\mathbf{y}}$ from (1) into the N-dimensional vector

$$\mathbf{y} = \sqrt{E_s}\, b\mathbf{h} + \mathbf{n}, \tag{59}$$

where

$$\mathbf{y} \overset{\Delta}{=} \mathbf{U}_N^H \tilde{\mathbf{y}}, \quad \mathbf{h} \overset{\Delta}{=} \mathbf{U}_N^H \tilde{\mathbf{h}}, \quad \mathbf{n} \overset{\Delta}{=} \mathbf{U}_N^H \tilde{\mathbf{n}}. \tag{60}$$

This represents a truncated Karhunen–Loeve Transform (KLT) (Jelitto & Fettweis, 2002, p. 21) (Hottinen *et al.*, 2003, p. 224), i.e., the optimum decorrelating transform, packing the largest amount of average intended-signal power from the original L-dimensional signal vector $\tilde{\mathbf{y}}$ into the N-dimensional vector $\mathbf{y}$ (Alouini *et al.*, 2000, Section 3.1) (Hottinen *et al.*, 2003, p. 224) (Jelitto & Fettweis, 2002, p. 21), which is desirable for dimension reduction.

- The components of the post-KLT signal vector $\mathbf{y}$ are linearly combined so as to maximize the conditioned output SNR (i.e., the maximal-ratio criterion (Brennan, 2003) using

$$\mathbf{w}_{MREC} = \mathbf{h}. \tag{61}$$

Recovery of a BPSK transmitted symbol, for instance, is attempted with

$$\hat{b}_{MREC} \quad = \quad sign\{\Re\left[\mathbf{w}_{MREC}^H \mathbf{y}\right]\} = sign\{\Re\left[\mathbf{h}^H \mathbf{y}\right]\}. \tag{62}$$

Eigencombining

Since eigencombining unifies the core principles of statistical beamforming and diversity combining, MREC is referred to as a superset of BF and MRC. Actually, $\text{MREC}_{N=1}$ represents **statistical beamforming (BF)**, whereas **maximal-ratio combining (MRC)** is equivalent with *full MREC*, i.e., $\text{MREC}_{N=L}$ (Alouini *et al.*, 2000, Section 4.2) (Dong & Beaulieu, 2002, Section II.A) (Siriteanu, 2006, Section 3.9.3) (Siriteanu & Blostein, 2007, Section III.D.2). Thus, any performance measure expression derived for MREC can be specialized to BF and MRC.

The components of $\mathbf{y}$ from (59), denoted hereafter as *eigenbranches*, are given by

$$y_i \overset{\Delta}{=} \mathbf{u}_i^H \, \tilde{\mathbf{y}} = \sqrt{E_s} \, b \, h_i + n_i, \, \forall i = 1 : N, \tag{63}$$

where

$$h_i \overset{\Delta}{=} \mathbf{u}_i^H \, \tilde{\mathbf{h}}, \quad n_i \overset{\Delta}{=} \mathbf{u}_i^H \, \tilde{\mathbf{n}}. \tag{64}$$

The components of $\mathbf{h}$, h_i, $i = 1 : N$, are hereafter referred to as channel *eigengains*. For our assumptions, the eigengains have zero mean. They are mutually uncorrelated because

$$E\{h_i h_j^*\} = \mathbf{u}_i^H \, E\{\tilde{\mathbf{h}}\tilde{\mathbf{h}}^H\} \, \mathbf{u}_j = \mathbf{u}_i^H \, \mathbf{R}_{\tilde{\mathbf{h}}} \, \mathbf{u}_j = \mathbf{u}_i^H \left(\sum_{l=1}^{L} \lambda_l \mathbf{u}_l \mathbf{u}_l^H \right) \mathbf{u}_j = \sum_{l=1}^{L} \lambda_l \mathbf{u}_i^H \, \mathbf{u}_l \mathbf{u}_l^H \, \mathbf{u}_j = 0, \quad \forall i \neq j, \tag{65}$$

and have autocorrelations (variances) given by

$$\sigma_{h_i}^2 \overset{\Delta}{=} E\{|h_i|^2\} = \mathbf{u}_i^H \, E\{\tilde{\mathbf{h}}\tilde{\mathbf{h}}^H\} \mathbf{u}_i = \mathbf{u}_i^H \left[\sum_{l=1}^{L} \lambda_l \mathbf{u}_l \mathbf{u}_l^H \right] \mathbf{u}_i = \sum_{l=1}^{L} \lambda_l \mathbf{u}_i^H \, \mathbf{u}_l \mathbf{u}_l^H \, \mathbf{u}_i = \lambda_i, \tag{66}$$

for any fading distribution (Alouini *et al.*, 2000). Thus,

$$\mathbf{R}_{\mathbf{h}} \overset{\Delta}{=} E\{\mathbf{h}\mathbf{h}^H\} = \mathbf{\Lambda}_N = diag\{\lambda_i\}_{i=1}^{N}. \tag{67}$$

Initial assumptions of Rayleigh fading and ZMCSCG noise yield

$$\mathbf{h} \sim \mathcal{N}_C(\mathbf{0}, \mathbf{\Lambda}_N), \tag{68}$$

so that the eigengains are independent, and

$$\mathbf{n} \sim \mathcal{N}_c(\mathbf{0}, N_0 \mathbf{I}_N), \tag{69}$$

so that the post-KLT noise is spatially (as well as temporally) white.

As mentioned earlier, $\mathbf{\Lambda}_L$ and $\mathbf{U}_L$ are hereafter assumed perfectly known. For the performance analysis shown below, the eigengains are also assumed perfectly known.

Table 2. Per-symbol **numerical complexity** *(no. of complex multiplications/additions)*

Implementation	Interpolation	MRC	BF	Ratio, for $L = 4$, $T = 11$
Suboptimum	SINC	$L(T+1)$	$(L + T + 1)$	3
	MMSE	$L(LT + 1)$	$(L + T + 1)$	11.25
Optimum	SINC	$L(L + T + 1)$	$(L + T + 2)$	3.75
	MMSE	$L(LT + L + 1)$	$(L + T + 2)$	11.5

Conditioned Output SNR

The conditioned SNR of the *i*th eigenbranch described by (63) is given by

$$\gamma_i \overset{\Delta}{=} \frac{E_s}{N_0} |h_i|^2, \quad i = 1:N. \tag{70}$$

Since $h_i \sim \mathcal{N}_c(0, \lambda_i)$, the distribution of γ_i is $\chi^2(2)$ or exponential, with average

$$\Gamma_i \overset{\Delta}{=} E\{\gamma_i\} = \frac{E_s}{N_0}\lambda_i$$

and variance Γ_i^2. The p.d.f., c.d.f., and m.g.f. for the eigenbranch conditioned SNRs have expressions analogous to those for SISO shown in (20), (21), and (26), respectively. Importantly, γ_i, $i = 1 : N$, are mutually independent.

As done for MRC in the derivation of (45), it can be shown for MREC that $\mathbf{w}_{MREC}$ from (61) maximizes the **conditioned output SNR**, i.e.,

$$\gamma = \sum_{i=1}^{N} \gamma_i, \tag{71}$$

justifying the title of *maximal-ratio eigencombining.*

Array Gain and Amount of Fading

The MREC **average output SNR** is then

$$\Gamma \overset{\Delta}{=} E\{\gamma\} = \sum_{i=1}^{N} \Gamma_i. \tag{72}$$

The **array gain**—defined in (36), for BF—can be written as follows for MREC and identically distributed channel gains,

i.e, for $\sigma_{\tilde{h}_i}^2 = \sigma_0^2 = \frac{1}{L} tr\mathbf{R}_{\tilde{\mathbf{h}}}$, $i = 1 : L$:

$$G_{A,MREC,N,dB} \overset{\Delta}{=} 10\log_{10}\frac{\Gamma}{\Gamma_0} = 10\log_{10}\left[L\left(\frac{\sum_{i=1}^{N}\lambda_i}{\sum_{i=1}^{L}\lambda_i}\right)\right] \in [10\log_{10}N, 10\log_{10}L]. \tag{73}$$

The lower and upper bounds are attained for uncorrelated and coherent channel gains, respectively. For BF, i.e., for $MRC_{N=1}$, Eqn. (73) yields $G_{A,BF,dB} \in [0, 10\log_{10}L]$, i.e., (38). For MRC, i.e., for $MREC_{N=L}$, Eqn. (73) yields $G_{A,MRC,dB} = 10\log_{10}L$, irrespective of the channel gain correlations, as already discussed.

To examine the fading-reduction capabilities of MREC, the **amount of fading** (AF)—defined in (50)—is now computed for the MREC output. Using the statistical independence of the individual eigenbranch SNRs, the variance of the MREC conditioned output SNR from (71) can be found as:

$$\sum_{i=1}^{N} \Gamma_i^2 .$$

Then, for the MREC AF we can write:

$$\frac{1}{N} \le AF_{MREC,N} = \frac{\sum_{i=1}^{N} \Gamma_i^2}{\left(\sum_{i=1}^{N} \Gamma_i\right)^2} = \frac{\sum_{i=1}^{N} \lambda_i^2}{\left(\sum_{i=1}^{N} \lambda_i\right)^2} \le 1. \tag{74}$$

According to Cauchy's inequality (Abramowitz & Stegun, 1995, §3.2.9, p. 11), the lower bound is achieved for identically distributed eigenbranches, i.e., when $\lambda_i = \lambda$, $\forall\ i = 1 : N$. For $N = L$, Proposition 2 indicates that the lower bound is achieved for i.i.d. channel gains, confirming that MRC of L branches reduces the fading severity vs. SISO by a factor of L. The upper bound in (74) is achieved when $\lambda_1 \neq 0$ and $\lambda_i = 0$, $\forall\ i = 2 : L$, i.e., for coherent channel gains. For $N = 1$, Eqn. (74) confirms that BF does not reduce fading.

Conditioned Output SNR Probability Density Function

Since the eigengains are independent, Eqns. (71) and (26) readily yield the m.g.f. of γ as

$$M_\gamma(s) = \prod_{i=1}^{N} \frac{1}{1 - s\Gamma_i}. \tag{75}$$

To simplify subsequent mathematical manipulation, let us hereafter employ the Laplace transform (Abramowitz & Stegun, 1995, §29.1.1, p. 1020) of the p.d.f. of γ, i.e., $F_\gamma(s) \overset{\Delta}{=} M_\gamma(-s)$, which we refer to as the *reversed moment generating function* (r.m.g.f.) of γ.

Eigenvalues of $\mathbf{R}_{\tilde{\mathbf{h}}}$ can become (nearly) equal, e.g., for certain AS values, as shown in Figures 1 and 6. Therefore, let $\{\Xi_1, \Xi_2, \ldots, \Xi_{N_d}\}$ denote the distinct values in the set of eigenbranch average SNRs $\{\Gamma_1, \Gamma_2, \ldots, \Gamma_N\}$. Then, Eqn. (75) yields

$$F_\gamma(s) = \prod_{k=1}^{N_d} \frac{1}{(1 + s\Xi_k)^{r_k}}, \tag{76}$$

where r_k represent the algebraic multiplicities of Ξ_k, $k = 1{:}N_d$, with

$$\sum_{k=1}^{N_d} r_k = N.$$

The r.m.g.f. from (76) can be expressed as (Siriteanu, 2006, Eqn. (3.165), p. 114)

$$F_\gamma(s) = \frac{1}{A} \sum_{k=1}^{N_d} \sum_{l=1}^{r_k} c_{k,l} \frac{1}{\left(s + \frac{1}{\Xi_k}\right)^l}, \tag{77}$$

where $A \overset{\Delta}{=} \prod_{k=1}^{N_d} \Xi_k^{r_k} = \prod_{i=1}^{N} \Gamma_i$, and the factor $c_{k,l}$ is given by (Siriteanu, 2006, Eqn. (3.166), p. 114)

$$c_{k,l} = (-1)^{r_k - l} \cdot \sum_{\Omega_i} \prod_{\substack{j=1 \\ j \neq k}}^{N_d} d_j \cdot \left(\frac{1}{\Xi_j} - \frac{1}{\Xi_k}\right)^{-(r_j + i_j)}, \tag{78}$$

for $k = 1{:}\,N_d$, $l = 1{:}\,r_k$, where Ω_i stands for the set of integers

$$\{i_j, j = 1{:}\,N_d, j \neq k \mid 0 \leq i_j \leq r_k - l, \sum_{\substack{j=1 \\ j \neq k}}^{N_d} i_j = r_k - l\},$$

and

$$d_j = \frac{(r_j - 1 + i_j)!}{(r_j - 1)! i_j!}$$

is the binomial coefficient.

The inverse Laplace transform of (77) yields for the p.d.f. of the MREC **conditioned output SNR** γ the following closed-form (Siriteanu, 2006, Eqn. (3.169), p. 115)

$$p(\gamma) = \frac{1}{A} \sum_{k=1}^{N_d} \sum_{l=1}^{r_k} c_{k,l} \cdot \frac{\gamma^{l-1} e^{-\gamma/\Xi_k}}{(l-1)!}, \tag{79}$$

by using (Abramowitz & Stegun, 1995, §29.3.10, p. 1022). This expression applies for correlated branches even when some eigenvalues are equal. Furthermore, for $L = 1$ (79) describes SISO, for $N = 1$ it describes BF, and for $N = L$ it describes MRC. When all eigenvalues are distinct, this reduces to (Lee, 1982, Eqn. 10-60, p. 308).

Figure 7 shows conditioned-SNR p.d.f. plots — obtained using (79) — for SISO and a $\mathrm{MREC}_{N=1:L}$ ULA with L= 5, for equal average output SNR of 10 dB, and Laplacian p.a.s. with $\theta_c = 0$ and $AS = 10^\circ$. The plots indicated with MREC, N = 1, and MREC, N = 5, represent BF and MRC, respectively. Since the AS is nonzero, $\mathrm{MREC}_{N=2:L}$ benefits from diversity gain, which changes the p.d.f. plot shape compared to SISO and BF (i.e., the p.d.f. peaks at non-zero SNR). Note that the p.d.f.s for $\mathrm{MREC}_{N=3:L}$ nearly overlap, suggesting that MRC-like performance is achievable with low-order MREC.

Outage Probability

The c.d.f. of γ can now be obtained from (79) as

$$P(\gamma) = \frac{1}{A} \sum_{k=1}^{N_d} \sum_{l=1}^{r_k} c_{k,l} \Xi_k^l \left[1 - e^{-\gamma/\Xi_k} \sum_{n=1}^{l} \frac{(\gamma/\Xi_k)^{n-1}}{(n-1)!} \right]. \tag{80}$$

A widely-applicable outage probability (OP) closed-form expression for MREC (BF, MRC), given the threshold SNR γ_{th}, results then from

$$P_o \overset{\Delta}{=} Pr(\gamma \leq \gamma_{th}) = P(\gamma_{th}). \tag{81}$$

Average Error Probability

The procedure used to derive the MRC AEP expression from (54) for uncorrelated branches, along with (75) and (76), yields the following MREC AEP expression for M–PSK (Alouini *et al.*, 2000, Eqn. (21)) (Siriteanu, 2006, Eqn. (3.151), p. 109):

$$P_{\mathrm{e,MREC,N}} = \frac{1}{\pi} \int_0^{\frac{M-1}{M}\pi} F_\gamma \left(\frac{g_{PSK}}{\sin^2\phi} \right) d\phi = \frac{1}{\pi} \int_0^{\frac{M-1}{M}\pi} \prod_{i=1}^{N} \left(1 + \Gamma_i \frac{g_{PSK}}{\sin^2\phi} \right)^{-1} d\phi \tag{82}$$

Figure 7. The p.d.f. of the conditioned output SNR for SISO and for a MREC$_{N=1:L}$ ULA with L = 5, for $AS = 10^\circ$ *and* $\Gamma_0 = \sum_{i=1}^{L} \widetilde{\Gamma}_i = 10$ *dB.*

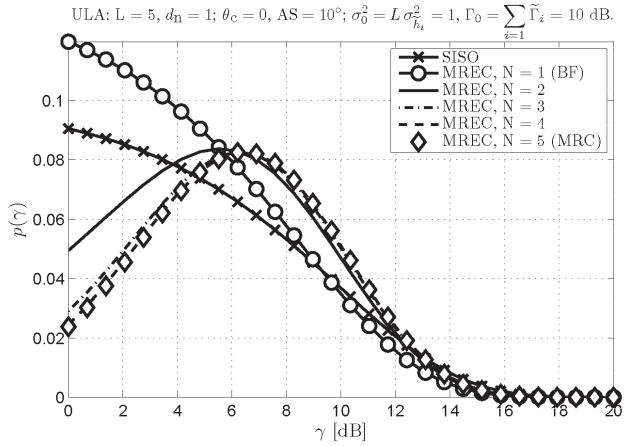

This nonclosed-form, finite-limit integral expression for the average **error probability** can be easily evaluated numerically. Now, using (77), the above can be recast as (Siriteanu, 2006, Eqn. (3.167), p. 114)

$$P_{\text{e,MREC,N}} = \frac{1}{A}\sum_{k=1}^{N_d}\sum_{l=1}^{r_k} c_{k,l}\cdot \Xi_k^l \cdot I_l(\Xi_k), \tag{83}$$

where (Siriteanu, 2006, Eqn. (3.168), p. 114)

$$I_l(\Xi_k) \overset{\Delta}{=} \frac{1}{\pi}\int_0^{\frac{M-1}{M}\pi} \left[1 + \Xi_k \frac{g_{PSK}}{\sin^2\phi}\right]^{-l} d\phi \tag{84}$$

is expressible in closed-form as in (Siriteanu, 2006, Section 3.10.2.1) based on (Simon & Alouini, 2000, Eqns. (5A.17–19), pp. 127–128). Note that (83) is not as straightforward to program on a computer as (82), because the factors $c_{k,l}$ given by (78) depend on the relative magnitudes of the eigenvalues of $\mathbf{R}_{\tilde{\mathbf{h}}}$.

Bear in mind that all the performance measure expressions derived above for MREC apply to SISO, BF, and MRC for $L = 1$, $N = 1$, and $N = L$, respectively. For correlated channel gains, the analysis of MRC based on its equivalence with full MREC is, due to the decorrelating effect of the KLT, much simpler than the analysis of MRC considered on its own (Alouini *et al.*, 2000; Dong & Beaulieu, 2002; Siriteanu & Blostein, 2007).

Performance Comparison

For unit-variance channel gains consider SISO and a BF, MREC, and MRC ULA with $L = 3$ for the following two cases:

- $AS_1 = 0$, i.e., coherent channel gains; then, the first row and the eigenvalue matrix of (Toeplitz) $\mathbf{R}_{\tilde{\mathbf{h}}}$ are given by $\left(\mathbf{R}_{\tilde{\mathbf{h}}}\right)_{1,j=1:L} = [1 \quad 1 \quad 1]$ and $\Lambda_L = \text{diag}\{3, 0, 0\}$.

- $AS_2 = 15^\circ$; then, $\left(\mathbf{R}_{\tilde{\mathbf{h}}}\right)_{1,j=1:L}$ = [1. 0.76 0.42] and $\mathbf{\Lambda}_L$ = diag{2.30, 0.58, 0.12}.

Figure 8 displays the AEPs computed using (82). For coherent branches, BF, MREC$_{N=2}$, and MRC actually coincide. There is maximum array gain, i.e., $10\log_{10}L \approx 4.8$ dB, over SISO, but no diversity gain. However, BF provides maximum array gain only for $AS_1 = 0^\circ$. Increasing AS diminishes the correlation between the channel gains, which decreases the correlation between the channel gains and the corresponding BF weights, and thus the array gain. For $AS_2 = 15^\circ$ the array gains computed with (73) are as follows: 3.6 dB for BF, 4.6 dB for MREC$_{N=2}$, and 4.8 dB (maximum) for MRC. The respective **amounts of fading**, computed using (74), are as follows: 1, 0.68, and 0.63. Thus, MREC$_{N=2}$ yields most of the available array gain, and about 1 dB more than BF. Note that the BF AEP plot remains parallel to that of SISO, even for non-zero AS, confirming a unit diversity order. MRC always performs best, due to maximum array and diversity gains. MREC$_{N=2}$ outperforms BF, because it yields more array gain as well as significant **diversity gain**. Actually, for small γ_b, MREC$_{N=2}$ approaches MRC in performance.

Simulation results are not shown here. Nevertheless, Figure 3.6 from (Siriteanu, 2006, p. 80) shows close agreement between the average error rates obtained from simulation and from (82), and confirms that the performance of MRC coincides with that of full MREC.

Figure 9 depicts the AEP for QPSK computed with (82), vs. AS, for SISO and for BF, MRC, and MREC ULA with L = 3, for unit-variance channel gains and γ_b= 5 dB. BF performance degrades with AS increasing around 0, unlike that of MREC$_{N>1}$. Furthermore, for $AS < 10^\circ$, near-MRC performance can be achieved with MREC$_{N=2}$. For estimated eigen/gains, analysis, simulation, and FPGA-based fixed-point-implementation results from (Siriteanu & Blostein, 2004; Siriteanu *et al.*, 2006; Siriteanu, 2006; Siriteanu & Blostein, 2007) suggest that MREC of carefully-selected small order can yield MRC-like performance, i.e., much better performance than BF.

Numerical Complexity Comparison

Let us compare the BF, MRC, and MREC numerical complexities for SINC/MMSE PSAM eigen/gain estimation and sub/optimum combining implementation — see (Siriteanu & Blostein, 2004; Siriteanu, 2006; Siriteanu & Blostein, 2007) for more details on these estimation and implementation techniques.

Unlike the channel gains, $\tilde{h}_i$, i =1 : L, required for actual MRC, the eigengains, h_i, i = 1 : N, required for BF or MREC, are always uncorrelated, and therefore they are estimated separately, at lower complexity. Then, the numerical complexity of MREC$_N$ (excluding the eigendecomposition, for the reasons explained earlier) is simply N times that of BF shown in Table 2 — see also (Siriteanu & Blostein, 2007, Table II).

For the example case with L = 5, T = 11, Table 2 indicates that suboptimum MRC (Siriteanu, 2006, Section 3.7.2) (Siriteanu & Blostein, 2007, Section III.C.1) is about 4.7 times more complex with MMSE PSAM than with SINC PSAM. This is because correlated fading requires joint estimation of $\tilde{h}_i$, i = 1 : L, for MMSE PSAM, but not for SINC PSAM (Siriteanu, 2006, Section 3.6.2). For optimum implementation (Siriteanu, 2006, Appendix A), MRC is about 3.5 times more complex with MMSE PSAM than with SINC PSAM. On the other hand, SINC and MMSE PSAM-based MREC have the same complexity, for either optimum or suboptimum implementation. The KLT also makes similar the complexities of the MREC optimum (Siriteanu, 2006, Section 3.7.1) (Siriteanu & Blostein, 2007, Section III.D.1) and suboptimum implementations (Siriteanu, 2006, Section 3.7.2) (Siriteanu & Blostein, 2007, Section III.C.4).

Finally, for MMSE PSAM, L = 5, and T = 11, full MREC has about three times lower complexity than MRC, for either optimum or suboptimum implementation. Moreover, MREC$_{N=2}$ has eight times lower complexity than MRC. On the other hand, for SINC PSAM, although full MREC is slightly more complex than MRC, MREC$_{N=2}$ still offers about a two-fold complexity reduction vs. MRC.

SMARTER ANTENNA ARRAYS WITH ADAPTIVE MREC

MREC Order Selection

The benefits of eigencombining can only be obtained by appropriate order selection. The procedure is analogous to the water-filling-based selection of transmission eigendirections in transmit-side eigenbeamforming or precoding (Sampath *et al.*, 2005; Vu & Paulraj, 2006; Zhou & Giannakis, 2003). Signal power is transmitted along an eigenvector only if the

Figure 8. AEP computed with (82) for SISO and for BF, MREC, and MRC ULA with L = 3, for $AS_1 = 0^\circ$ *and* $AS_2 = 15^\circ$

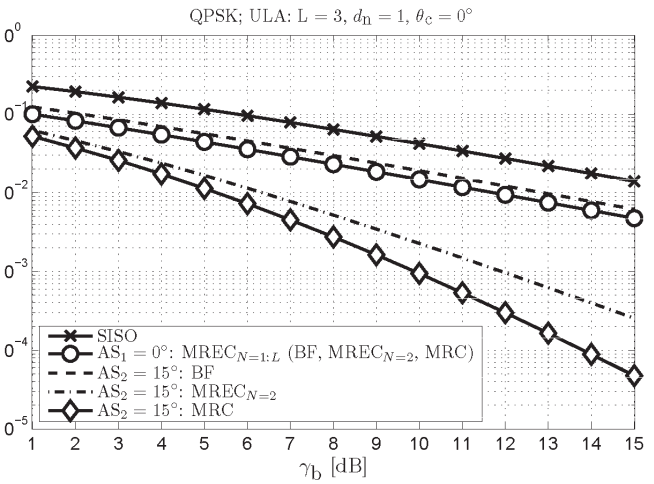

Figure 9. Top: AEP performance for QPSK, unit-variance channel gains, and average bit-SNR γ_b *= 5dB, for SISO and for BF, MRC, and MREC ULA with L = 3; Bottom: Correlations between the channel gains corresponding to adjacent and extreme antenna elements, and the eigenvalues of* $\mathbf{R}_{\tilde{\mathbf{h}}}$.

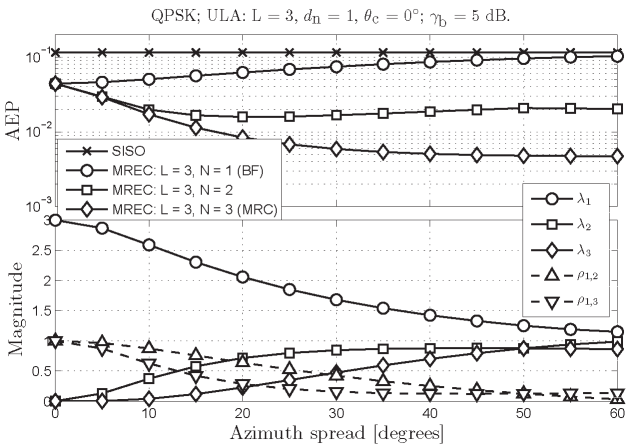

channel is "good" along it. However, the actual power-loading that occurs in transmit-side eigenbeamforming does not have a counterpart in receive-side eigencombining.

Consider the simple *bias–variance tradeoff criterion* (BVTC) (Jelitto & Fettweis, 2002, p. 22), wherein the MREC order is determined from

$$\min_{N=1:L} \left[E_s \cdot \sum_{i=N+1}^{L} \lambda_i + N_0 \cdot N \right] \cdot \tag{85}$$

Essentially, the BVTC balances the loss incurred by removing the weakest (L –N) intended-signal contributions (the first term) against the residual-noise contribution (the second term). The BVTC output depends on the relative magnitudes of the eigenvalues, i.e., on the spatial correlation, as well as on the symbol SNR, E_s / N_0. Order-selection criteria that

also depend on the actual channel estimation method, symbol-detection performance (or quality-of-service), and system load appear in (Siriteanu *et al.*, 2006; Siriteanu & Blostein, 2007). Coarse adaptation to the propagation conditions was proposed in (El Zooghby, 2005, p. 270) by means of switching between BF and MRC when correlation reaches 0.5.

Adaptive-MREC Performance and Complexity for Random Azimuth Spread

We generated 10,000 independent azimuth spread (AS) samples from the lognormal distribution described by (17) for the typical urban scenario described in Table 1, for which the **power azimuth spectrum** (p.a.s.) is Laplacian — see (15). The AS sequence mean and standard deviation were about 9.81° and 13.40°, respectively, and $Pr(1^\circ \le AS \le 20^\circ) \approx 0.82$. For each AS sample, expression (82) was used to compute the AEP for SISO and for BF, BVTC-based adaptive MREC, and MRC ULA with $L = 5$, for QPSK and perfectly known channel. The means of these AEPs over the AS samples are shown in the top subplot of Figure 10. The lower subplot displays the average MREC order output by the BVTC. Note first that for high enough average bit-SNR, γ_b, BF outperforms SISO by only about 5.5 dB, which implies a loss of array gain for BF of about $10\log_{10}L - 5.5 \approx 1.5$ dB due to imperfect coherence between the channel gains and the applied BF combiner. MRC outperforms BF by the diversity gain, which increases with increasing γ_b. On the other hand, adaptive MREC approaches BF and MRC in performance at low and high SNR, respectively, because the BVTC outputs increasing MREC order with increasing SNR.

Similar results appear for BPSK, MMSE PSAM channel estimation, and optimum combining implementation in (Siriteanu & Blostein, 2007, Figure 2). There, for $\gamma_b = 4$ dB, the average BVTC output is $N = 2$, which makes MREC two times more complex than BF and eight times less complex than MRC, as discussed earlier. On the other hand, $\gamma_b = 4$ dB yields $AEP = 2 \cdot 10^{-2}$ for $\text{MREC}_{N=2}$. For $AEP \approx 2 \cdot 10^{-2}$, adaptive MREC outperforms BF by more than 3 dB, and is outperformed by MRC by less than 0.5 dB.

Figure 11 displays for a typical urban scenario the following numerical results: 1) Lognormal **AS** samples generated using (17), with spatial (or, equivalently, temporal) correlation given by (18), when the subscriber moves over the distance shown on the abscissa; 2) The corresponding QPSK AEPs for SISO and for BF, BVTC-based adaptive MREC, and MRC ULA with $L = 5$, for $\gamma_b = 5$ dB, perfectly known channel, and Laplacian p.a.s.; and 3) The MREC order output by the BVTC, vs. time. These results indicate that adaptive MREC performs nearly as well as MRC (and thus much better than BF), while processing fewer dimensions most of the time. For BPSK, MMSE PSAM, and optimum combining implementation, similar results appear in (Siriteanu & Blostein, 2007, Figure 3).

For FPGA-based implementations, (Siriteanu et al., 2006) found that adaptive MREC yields near-MRC performance while doubling the number of subscribers simultaneously processed with the same baseband resources at the base-sta-

Figure 10. Top: Mean AEP computed with (82) for QPSK, SISO and BF, BVTC MREC, and MRC ULA with L = 5, obtained by averaging over 10000 lognormal AS samples, for a base-station in a typical urban scenario. Bottom: Mean MREC order selected with the BVTC criterion.

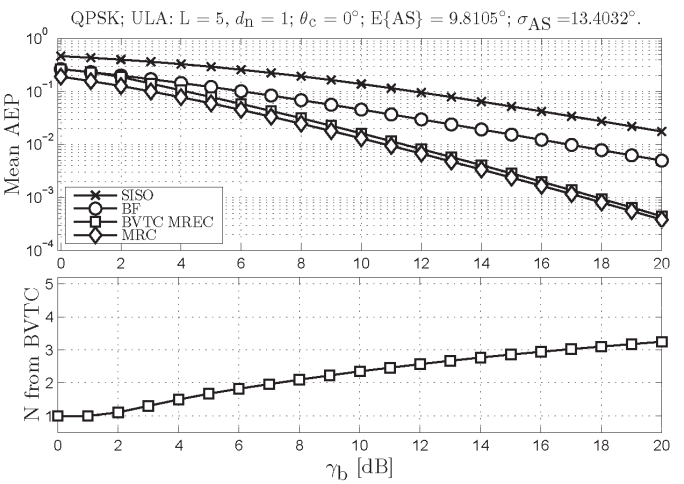

Figure 11. Top: Base-station AS vs. distance traveled by the subscriber, for a typical urban scenario; Middle: AEP computed for QPSK with (82), for SISO and BF, BVTC MREC, and MRC ULA with L = 5, for γ_b = 5 dB; Bottom: MREC order N selected with the BVTC, vs. time.

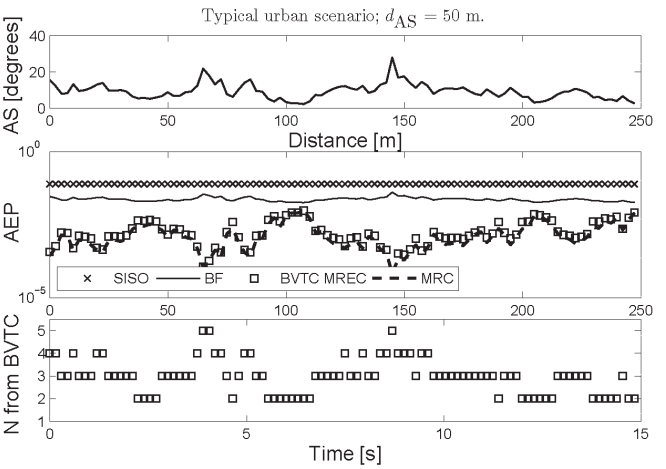

tion. Resources wasted with MRC on low-AS subscribers can with adaptive MREC benefit high-AS subscribers. Thus, adaptive MREC can efficiently benefit from *azimuth spread diversity.*

In conclusion, through its adaptability to channel propagation and noise conditions — as well as to subscriber quality-of-service and system processing power limitations (Siriteanu *et al.*, 2006; Siriteanu & Blostein, 2007) — MREC closes the performance and complexity gaps between BF and MRC, and eliminates the unwarranted risks and costs of their stand-alone deployments.

RELATED APPLICATIONS AND FURTHER RESEARCH

For the numerical results shown in this chapter we have simulated AS values similar to those measured in actual urban scenarios at the base station (Algans *et al.*, 2002; Vaughan & Andersen, 2003). Nevertheless, multi-antenna transceivers are also envisioned at the subscriber stations (El Zooghby, 2005, Chapter 9), although there adoption pace is slow, due to high cost and power consumption (Hottinen *et al.*, 2006). Although the subscriber station typically experiences much higher AS than the base station (3GPP, 2003, Table 4.1) (El Zooghby, 2005, Sections 3.6.5, 9.2), the limited size of the former restricts antenna array interelement distance to values that may yield channel gain correlations (3GPP, 2003, Table 4.2) that are too large for MRC and too small for BF. Higher returns may then be possible with adaptive MREC that finely matches the actual channel and noise conditions, compared to switching between BF and MRC for a certain correlation threshold (El Zooghby, 2005, p. 270).

Throughout this chapter, we have analyzed the BF, MRC, and adaptive MREC performance for receiving antenna array receivers (i.e., SIMO systems) assumed to have perfect channel knowledge, and have compared their numerical complexities for estimated fading. The BF, MRC, and adaptive MREC performance is analyzed for imperfectly known fading as well as for optimum and suboptimum combining implementations in (Siriteanu & Blostein, 2004; Siriteanu, 2006; Siriteanu & Blostein, 2007). Performance and resource usage evaluations for a fixed-point FPGA-based implementation appear in (Siriteanu *et al.*, 2006). A description of optimum eigencombining implementation for interference-limited systems appears in (Siriteanu, 2006, Section 6.5.4). Simulation results for SIMO eigencombining for interference-limited scenarios and estimated channel eigenstructure are shown in (Brunner *et al.*, 2001).

An interesting issue that has been pointed out in (Siriteanu & Blostein, 2004) (Siriteanu & Blostein, 2007, Section III.C), and should be given further consideration, is that, for the practical case of suboptimum channel estimation and suboptimum combining implementation, MREC can actually outperform MRC. Thus, knowledge of channel eigendecomposition — which can be estimated more accurately than the actual channel gains, especially in high-mobility

scenarios (Brunner *et al.*, 2001; Vu & Paulraj, 2006) — can in practice not only reduce complexity, but even enhance the performance. This effect is more pronounced at high spatial correlation and low SNR (F. A. Dietrich & Utschick, 2003, Figure 2) (Jelitto & Fettweis, 2002, Figure 6) (Siriteanu & Blostein, 2004, Figures 2, 3, 4, 7). Further research is also necessary on order selection criteria that have recently been proposed in (F. Dietrich & Utschick, 2002) (Siriteanu et al., 2006) (Siriteanu & Blostein, 2007).

Although in this chapter we have illustrated the performance of eigencombining only for spatial receivers and have not considered interference, other applications and extensions are possible. Consider first the Rake receivers (Patenaude *et al.*, 1999; Simon & Alouini, 2000) typically deployed in CDMA systems. There, high intertap correlation found by measurements has indicated that the "effective diversity is ... significantly lower than the number of maxima in the power delay profile" (Patenaude *et al.*, 1999, p. 605). Adaptive eigencombining may thus greatly extend subscriber station battery life, as well as allow base stations to process significantly more subscribers for a given deployment and operational cost, compared to MRC. Furthermore, since azimuth spread and delay spread are correlated (Algans *et al.*, 2002, Section VI.B), joint eigencombining across antennas and Rake taps is another interesting research direction.

Finally, more realistic eigencombining performance evaluations should utilize recently-documented relationships among azimuth spread, delay spread, and fading distribution type. For example, it would be worth investigating Rice or Nakagami fading models with parameters determined from the azimuth and delay spread.

SUMMARY AND CONCLUSION

The chapter has provided an introduction to principal signal processing methods employed for receive-side smart antenna technology. We have compared statistical beamforming (BF) and maximal-ratio combining (MRC) with the conventional single-antenna transceiver, and have found that great performance benefits are achievable due to array and diversity gain, in favorable propagation conditions. For unfavorable conditions, BF and MRC performance can hardly justify their deployment and operational costs. Furthermore, although their numerical complexity remains fixed, BF and MRC performance fluctuates when propagation conditions vary as in actual scenarios.

Instead of BF and MRC, adaptive eigencombining should be considered in the development of smarter antenna technologies. Maximal-ratio eigencombining (MREC) unifies the signal processing principles and analyses of BF and MRC. Expressions for symbol-detection performance measures such as the outage probability and average error probability have been derived that apply throughout the fading correlation range. Numerical results presented for realistic scenarios demonstrate the performance-improving and complexity-reducing benefits of adaptive MREC over conventional BF or MRC.

REFERENCES

3GPP. (2003). *Technical Specification Group Radio Access Network. Spatial Channel Model for Multiple Input Multiple Output (MIMO) Simulations, Release 6* (Tech. Rep. No. TS 25.996). 3rd Generation Partnership Project (3GPP).

Abramowitz, M., & Stegun, I. A. (Eds.). (1995). *Handbook of mathematical functions with formulas, graphs and mathematical tables.* New York, NY 10014: Dover Publications, Inc.

Algans, A., Pedersen, K. I., & Mogensen, P. E. (2002, April). Experimental analysis of the joint statistical properties of azimuth spread, delay spread, and shadow fading. *IEEE Journal on Selected Areas in Communications, 20*(3), 523-531.

Alouini, M.-S., Scaglione, A., & Giannakis, G. B. (2000, September). PCC: principal components combining for dense correlated multipath fading environments. In *Proc. IEEE vehicular technology conference, (VTC '00)* (Vol. 5, p. 2510-2517).

Applebaum, S. (1976, September). Adaptive arrays. *IEEE Transactions on Antennas and Propagation, 24*(5), 585 - 598.

Bahrami, H. R., & Le-Ngoc, T. (2006, December). Precoder design based on correlation matrices for MIMO systems. *IEEE Transactions on Wireless Communications, 5*(12), 3579 - 3587.

Blogh, J. S., & Hanzo, L. (2002). *Third-generation systems and intelligent wireless networking: Smart antennas and adaptive modulation.* Chichester, West Sussex, England: John Wiley and Sons.

Brennan, D. G. (2003, February). Linear diversity combining techniques. *Proceedings of the IEEE, 91*(2), 331 - 356.

Brunner, C., Utschick, W., & Nossek, J. A. (2001). Exploiting the short-term and long-term channel properties in space and time: eigenbeamforming concepts for the BS in WCDMA. *European Transactions on Telecommunications. Special Issue on Smart Antennas*, 12(5), 365-378.

Choi, J., & Choi, S. (2003, May). Diversity gain for CDMA systems equipped with antenna arrays. *IEEE Transactions on Vehicular Technology, 52*(3), 720-725.

Choi, S., Choi, J., Im, H.-J., & Choi, B. (2002, September). A novel adaptive beamforming algorithm for antenna array CDMA systems with strong interferers. *IEEE Transactions on Vehicular Technology, 51*(5), 808-816.

Dietrich, F., & Utschick, W. (2002). On the effective spatio-temporal rank of wireless communication channels. In *Proc. 13th IEEE international symposium on personal, indoor and mobile radio communications, (PIMRC '02)* (Vol. 5, p. 1982-1986).

Dietrich, F. A., & Utschick, W. (2003, September). Maximum ratio combining of correlated Rayleigh fading channels with imperfectly known channel. *IEEE Communications Letters, 7*(9), 419-421.

Dong, X., & Beaulieu, N. (2002, January). Optimal maximal ratio combining with correlated diversity branches. *IEEE Communications Letters, 6*(1), 22-24.

El Zooghby, A. (2005). *Smart antenna engineering.* Norwood, MA: Artech House.

Ertel, R. B., Cardieri, P., Sowersby, K. W., Rappaport, T. S., & Reed, J. H. (1998, February). Overview of spatial channel models for antenna array communication systems. *IEEE Personal Communications,5*(1), 10 - 22.

Godara, L. C. (2004). *Smart antennas.* Boca Raton, FL: CRC Press.

Goldberg, J. M., & Fonollosa, J. R. (1998). Downlink beamforming for spatially distributed sources in cellular mobile communications. *Signal Processing, 65*(2), 181-197.

Golub, G. H., & Loan, C. F. van. (2000). *Matrix computations*. New York, NY: The John Hopkins University Press.

Hottinen, A., Kuusela, M., Hugl, K., Zhang, J., & Raghothaman, B. (2006, August). Industrial embrace of smart antennas and MIMO. *IEEE Wireless Communications, 13*(4), 8-16.

Hottinen, A., Tirkkonen, O., & Wichman, R. (Eds.). (2003). *Multi-antenna tranceiver techniques for 3G and beyond.* Chichester, West Sussex, England: John Wiley and Sons.

Jakes, W. C. (Ed.). (1974). *Microwave mobile communications.* New York, NY: John Wiley and Sons.

J. C. Liberti, J., & Rappaport, T. S. (1999). *Smart antennas for wireless communications: IS-95 and third generation CDMA applications.* Upper Saddle River, NJ: Prentice Hall PTR.

Jelitto, J., & Fettweis, G. (2002, December). Reduced dimension space-time processing for multi-antenna wireless systems. *IEEE Wireless Communications, 9*(6), 18-25.

Lee, W. C. Y. (1982). *Mobile communications engineering.* Englewood Cliffs, NJ: McGraw-Hill.

Monzingo, R. A., & Miller, T. W. (1980). *Introduction to adaptive arrays*. New York: John Wiley and Sons.

Patenaude, F., Lodge, J., & Chouinard, J.-Y. (1999, March). Eigen analysis of wide-band fading channel impulse responses. *IEEE Transactions on Vehicular Technology, 48*(2), 593 - 606.

Paulraj, A., Nabar, R., & Gore, D. (2005). *Introduction to space-time wireless communications.* Cambridge, UK: Cambridge University Press.

Pedersen, K. I., Mogensen, P. E., & Fleury, B. H. (2000, March). A stochastic model of the temporal and azimuthal dispersion seen at the base station in outdoor propagation environments. *IEEE Transactions on Vehicular Technology, 49*(2), 437-447.

Proakis, J. G. (2001). *Digital communications* (Fourth ed.). New York, NY: McGraw-Hill, Inc.

Rensburg, C. van, & Friedlander, B. (2004, November). Transmit diversity for arrays in correlated Rayleigh fading. *IEEE Transactions on Vehicular Technology, 53*(6), 1726-173.

Rooyen, P. van, Lotter, M., & Wyk, D. van. (2000). *Space-time processing for CDMA mobile communications.* Norwell, MA: Kluwer Academic Publishers.

Roy, R. H. (1998, March). An overview of smart antenna technology: the next wave in wireless communications. In *Proceedings of the IEEE Aerospace Conference, 1998* (Vol. 3, p. 339-345).

Salz, J., & Winters, J. H. (1994, November). Effect of fading correlation on adaptive arrays in digital mobile radio. *IEEE Transactions on Vehicular Technology, 43*(4), 1049-1057.

Sampath, H., Erceg, V., & Paulraj, A. (2005, March). Performance analysis of linear precoding based on field trials results of MIMO-OFDM system. *IEEE Transactions on Wireless Communications, 4*(2), 404-409.

Siemens. (2000). *Text proposal for RAN WG1 report on Tx diversity solutions for multiple antennas* (Tech. Rep. No. TSGR1#15 R1-00-1126). 3rd Generation Partnership Project (3GPP).

Simon, M. K., & Alouini, M.-S. (2000). *Digital communication over fading channels. A unified approach to performance analysis.* Baltimore, Maryland: John Wiley and Sons.

Siriteanu, C. (2006). *Maximal-ratio eigen-combining for smarter antenna array wireless communication receivers.* Unpublished doctoral dissertation, Queen's University, Kingston, Canada.

Siriteanu, C., & Blostein, S. D. (2004, January–April). Maximal-ratio eigencombining: a performance analysis. *Canadian Journal of Electrical and Computer Engineering, 29*(1/2), 15-22.

Siriteanu, C., & Blostein, S. D. (2007, March). Maximal-ratio eigen-combining for smarter antenna arrays. *IEEE Transactions on Wireless Communications, 6*(3), 917 - 925.

Siriteanu, C., Blostein, S. D., & Millar, J. (2006). FPGA-based communications receivers for smart antenna array embedded systems. *EURASIP Journal on Embedded Systems. Special Issue on Field- Programmable Gate Arrays in Embedded Systems, 2006*, Article ID 81309, 13 pages.

Stridh, R., Bengtsson, M., & Ottersten, B. (2006, April). System evaluation of optimal downlink beamforming with congestion control in wireless communication. *IEEE Transactions on Wireless Communications, 5*(4), 743 - 751.

Trees, H. L. V. (2002). *Optimum array processing: Part IV of detection, estimation, and modulation theory.* New York, NY: John Wiley & Sons, Inc.

Tse, D., & Viswanath, P. (2005). *Fundamentals of wireless communication.* Cambridge, UK: Cambridge University Press.

Vaughan, R., & Andersen, J. B. (2003). *Channels, propagation and antennas for mobile communications.* London: The Institution of Electrical Engineers.

Vu, M., & Paulraj, A. (2006, June). Optimal linear precoders for MIMO wireless correlated channels with nonzero mean in space-time coded systems. *IEEE Transactions on Signal Processing, 54*(6), 2318-2332.

Zhou, S., & Giannakis, G. B. (2003, July). Optimal transmitter eigen-beamforming and space-time block coding based on channel correlations. *IEEE Transactions on Information Theory, 49*(7), 1673 - 1690.